Generator Coherency Identification Method Based on Phase Trajectory Vector and Its Applications to Power System Transient Stability Control

September 2019

楊 松浩

Dedicated to my upcoming child.

Wish him/her healthy and happy!

Abstract

Generator Coherency (GC), which is defined as the similarity of generator angle curves after system suffers from large disturbances, plays a significant role in the power system stability assessment and control. The major difficulty of the work of Generator Coherency Identification (GCI) lies in two aspects, which are 1) the variation of GC due to the different system operating conditions and disturbances, and 2) the time-evolution of GC during the dynamic process.

To address the problems of GCI, a novel concept of Phase-plane Trajectory Vector (PTV) is proposed in this thesis. It can describe the dynamics of generators accurately with the aid of real-time measurement data from Phasor Measurement Units (PMUs). PTVs provide abundant information about generators' dynamics, which greatly improves the accuracy and speed of GCI. Compared with conventional GCI methods, PTV based GCI method can adapt to the different system operating conditions and disturbances. Besides, it can track the time-evolution of GC during the dynamic process. Moreover, PTV based method also has advantages of efficient computation and flexible application.

Due to above-mentioned advantages, PTVs are used for two different scenarios: 1) Critical Machines (CMs) identification for Transient Stability Assessment (TSA) and 2) dynamic GCI for Controlled Islanding (CI).

In the proposed CMs identification scheme for TSA, PTVs are used to describe the dynamics of generators and the K-means clustering algorithm is applied to identify CMs and Non-critical Machines (NMs). The simulations in IEEE 39-bus power system show that the proposed method is more accurate than conventional methods in general cases. Moreover, the PTV based method can track the time-evolution of CMs during the dynamic process.

In the proposed GCI scheme for CI, PTVs are used to describe the dynamics of generators and the hierarchical clustering algorithm is applied to determine the coherency of generators. Inspired by PTVs on the Phase Plane for Generators (PPG), a novel concept of Phase Plane for Buses (PPB) is proposed to determine the coherency of non-generator buses. The simulations show that the proposed GCI scheme can identify the dynamic coherency of generator and buses, and make proper islanding strategy according to current system states.

Keywords: Generator Coherency, Phase-plane Trajectory Vector, Transient Stability Assessment, Controlled Islanding, Power System Stability Assessment and Control

Acknowledgments

I would like to thank my supervisor Masahide Hojo at the University of Tokushima for invaluable support and help during the writing of the journal papers and this thesis. Your support has been a great source of input and motivation, and I thank you for taking the time to provide thoughtful guidance during my studying in Japan.

I would also like to extend my thanks to my colleagues, Hao Ma, and Xiao Yan. They gave me their friendly support and assistance during living at the University of Tokushima.

Finally, I would like to greatly thank my family, my respectable parents, my deep loved wife and upcoming child. Thanks for your support, understanding, and encouragement throughout all these years.

Achievements

Journal Papers

[1] **Yang S**, Hao Z, Zhang B et al. An Accurate and Fast Start-up Scheme for Power System Real-time Emergency Control[J]. IEEE Transactions on Power Systems, 2019. (In Press)

[2] **Yang S**, Zhang B, Hojo M et al. An ME-SMIB Based Method for Online Transient Stability Assessment of a Multi-Area Interconnected Power System[J]. IEEE Access, 2018,6:65874-65884.

[3] **Yang S**, Hojo M, Zhang B. A Phase-plane-based Dynamic Coherency Real-time Identification Scheme for Controlled Islanding[J]. IEEJ Transactions on Electrical and Electronic Engineering, 2019,14(4):561-568.

[4] **Yang S**, Hojo M, Zhang B. A Phase-Plane Trajectory Vector-Based Method for Real-Time Identification of Critical Machines[J]. IEEJ Transactions on Electrical and Electronic Engineering, 2018,13(11):1578-1585.

Conference Papers

[1] **Yang S**, Zhang B, Hojo M. A Dynamic Generator Coherency Identification Method Based on Phase Trajectory Vector[C]: 2018 IEEE Innovative Smart Grid Technologies-Asia (ISGT Asia), Singapore.

[2] **Yang S**, Zhang B, Hojo M et al. An Optimal Scheme for PMU Placement Based On Generators Grouping[C]: 2016 IEEE PES Asia-Pacific Power and Energy Engineering Conference (APPEEC), Xi'an, China.

Content

List of Tables

List of Figures

Figure 4-11 Areas Corresponding to Scenario 2 in Case 2

Abbreviations

COI	Centre Of Inertia
CG	Coherent Generator
CGG	Coherent Generator Group
COGG	Center Of Generator Group
CI	Controlled Islanding
CM	Critical Machine
EEAC	Extended Equal Area Criterion
E-SMIB	Equivalent Single-Machine Infinite Bus
GC	Generator Coherency
GCI	Generator Coherency Identification
LAG	Largest Angle Gap
NM	Non-critical Machine
PMU	Phasor Measurement Unit
PPB	Phase Plane for Buses
PPG	Phase Plane for Generators
PTV	Phase-plane Trajectory Vector
SEP	Stable Equilibrium Point
SIME	SIngle Machine Equivalent
SMIB	Single-Machine Infinite Bus
TSA	Transient Stability Assessment
UEP	Unstable Equilibrium Point
UFLS	Under Frequency Load Shedding
UVLS	Under Voltage Load Shedding
WAMS	Wide Area Measurement System

1 Introduction

1.1 Background

The vast growth of power demand and expansion of network have resulted in an ever-greater interconnected power system. In consideration of economy and efficiency, the bulk power system usually operates close to its limits, which greatly increases the risks of unpredicted disturbances[1]. The ability to resist disturbances and maintaining stability turns out to be crucial to power system operation. Consequently, a volume of work has been carried out on power system stability analysis, assessment, and control.

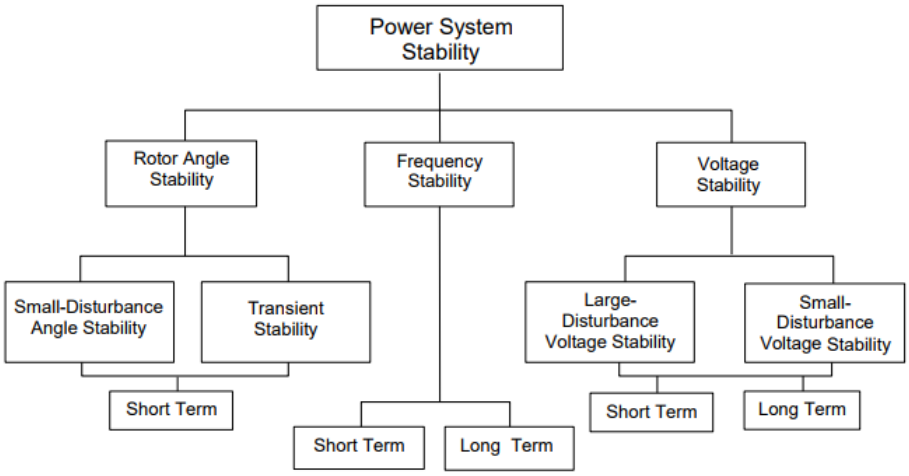

Figure 1-1 Classification of Power System Stability

Figure 1-1 gives the overall picture of the power system stability problems[2]. Among the above issues, the rotor angle stability is of vital importance for the synchronous AC power system. The transient angle stability refers to the ability to maintain synchronization among synchronous machines after the system suffers from large disturbances. Once the synchronization is lost, grid failure or even blackout will be caused[3]. To prevent the system from collapse, much work, such as the relays protections, transient stability assessment, emergency control, controlled islanding and so on, has been widely reported.

During the dynamic process of power system which is subjected to disturbances, synchronous generators are likely to behave in forms of several groups. In each group, generators have a similar

transient response and the similarity is called Generator Coherency (GC). Among all efforts to maintain the power system stability, generator coherency identification (GCI) is necessary from different perspectives[4]. For example, the critical machines identification, which is required in the power system transient stability assessment (TSA), is based on the results of GCI[5]. Moreover, GC is the essential requirement in controlled islanding strategy[6, 7]. Hence, it is of the essence to correctly identify GC in power system stability assessment and control.

1.2 Research status of GCI

The identification of coherent generators (CGs) is vitally important for the power system stability assessment and control. The purposes of GCI can be summarized into three categories.

a) System Dynamic Reduction

As the dynamics of CGs are similar during the transient process, the group of CGs can be represented by an equivalent generator. Partitioning the bulk power system into areas, and then replacing the areas with equivalent models can greatly simplify the transient simulation and analysis for a large-scale power system. Due to the significant improvement in computation efficiency, researches on system dynamic reduction which is based on the GC has been widely reported [8-13].

b) Wide-Area Measurement and Control

The wide-area measurement and control include the phasor measurement, state estimation[14-16], stability assessment[17] and control [4, 18, 19]of a power system in aid of the wide-area measurement system (WAMS). GCI can be used in the Wide-Area Measurement and control for different purposes. For example, the results of GCI can provide effective suggestions for damping the inter-area oscillations[19, 20]. And it can help determine the proper locations of PMU measurement devices[21-23]. Besides, GCI is necessary for transient stability assessment of power systems in Equivalent-Single Machine Infinite Bus(E-SMIB) based methods such as Extended Equal Area Criterion(EEAC)[24, 25], SIngle Machine Equivalent(SIME) method[26-28] and phase trajectory's concave-convexity based method[29-31].

c) Controlled Islanding

Controlled islanding (CI) is regarded as the last attempt to prevent the system from collapse[32]. It aims to separate the power system into multiple self-sustainable and controllable islands before the blackout occurs[33]. Among all technical requirements of CI, the GC is the first and most important one. It ensures that each island is sustainable and stable. GCI forms the basis for islanding process[4].

The key to achieving accurate GCI is the identification of similarity of generators' dynamic response. And the major difficulty of GCI lies in the variability of CGs. Firstly, the coherency of generators is different when the system is changed in disturbances, operation condition, system configuration [34].

Secondly, even for each scenario, the controllers of the power system such as generator regulators and relay protection also influence the dynamics of generators and change the coherency. Thus, an effective coherency identification method must consider the effects of the above factors. It should be able to adapt to different scenarios and to track the variation of coherency during the whole dynamic process.

To address this problem, a number of methods have been developed to identify the coherency of generators, which can be classified into two types: the model-based methods and measurement-based methods [35].

The model-based methods, such as the slow coherency technique[36, 37], can identify the coherency of generators based on the time-domain analysis on the linear dynamic model of power systems at a specific operating point. After disturbance occurs, those generators swinging together in a slow mode are identified as coherent. One major limitation of these methods is that the accuracy depends on the system models. Besides, the GCI results of these methods remain unchanged when the power system changes the operating conditions or suffers from different disturbances, which is not coincident with the practice. To address the problem, a continuation method is proposed in [38] to trace the loci of coherency indices of slow modes with respect to variation in system conditions. However, the effects of different disturbances are still not taken into consideration. What's more, the time-variation of GC during the dynamic process which is caused by the controllers and multiple disturbances are totally neglected. Due to these obvious limitations, the model-based methods are gradually replaced by the following measurement-based methods[11].

The measurement-based methods, which identify the generator coherency based on real-time measurement data, are greatly enhanced with the fast development of Phasor Measurement Units (PMUs) in the power system. These methods can adapt to various operation conditions, topology changes, and different disturbances by using the real-time measurement data because all the influences of these factors are reflected in the transient response of the power system. Due to the advantages over model-based methods, the measurement-based methods are attracting increasing attention in the area of GCI. This kind of methods are widely reported based on independent component analysis[39], support vector clustering[40], principal component analysis[41, 42], Koopman Mode Analysis[43], correlation characteristics[20], hierarchical cluster [44], Hilbert-Huang transform [45], spectral clustering method[32, 46-49], discrete Fourier transform [16], wavelet phase difference[50][51], artificial neural network[17], Lyapunov exponent[52], graph theory[7, 53], bio-inspired technology [54], projection pursuit [55] and so on. They can fast identify the coherency of generators with a short term of measurement data after the disturbances. However, these methods also have the limitations including (i) heavy computation burden, (ii) long-time window of data and (iii) inability to identify the dynamic coherency. Heavy computation

burden is related to the enormous offline training and massive data processing. The long-time window of data is the guarantee of the sufficient analysis of the time-domain or frequency-domain characteristics of generator coherency. The last but also the most important limitation is that these methods cannot identify the changes in generator coherency during the dynamic process. A promising method based on the frequency deviation signal was proposed to track the change of coherency time evolution in [34]. However, a sufficient time window of measurement data is still required. Besides, the coherency is difficult to identify at moments when the frequency deviations of different coherent groups are similar.

1.3 The application of GCI in power system stability assessment and control

In China power system practice, the rule of "Three Defense Lines" is essential to power system stability and control[56, 57]. Figure 1-2 presents a schematic diagram of the Three Defense Lines rule. The details are given as follows.

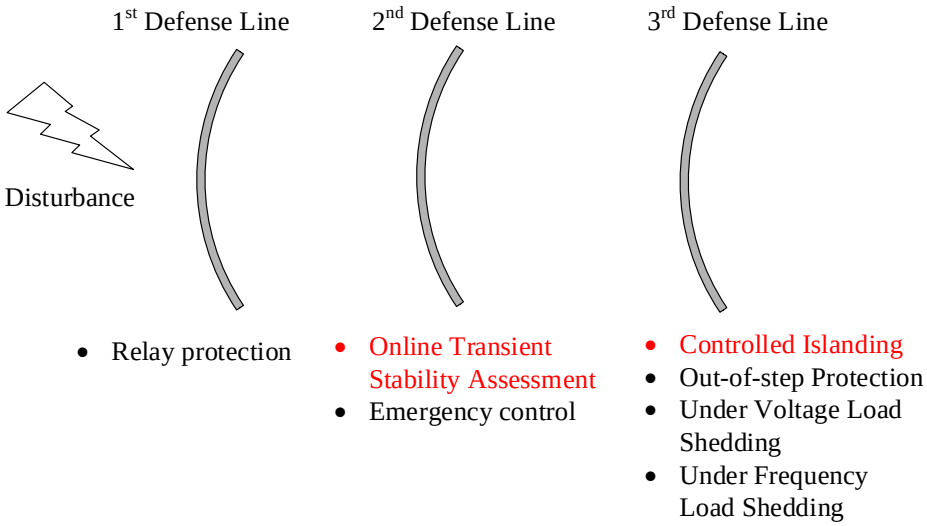

Figure 1-2 "Three Defence Lines" in China Power System Stability Control

a) 1st Defense Line

The 1st Defense Line consists of different relay protections, which are designed to eliminate the fault devices fast and accurately. It is the most straightforward and effective way to reduce the effects of the disturbances and enhance the transient stability of the power system.

b) 2nd Defense Line

The 2nd Defense Line consists of transient stability assessment and emergency control. It aims to guarantee the transient stability of power systems when subjected to large disturbances. The transient stability of the post-disturbance system is first evaluated by TSA methods. In some TSA methods, the GCI is of vital importance to obtain accurate TSA results. Once the system is detected or predicted as unstable,

the emergency control will launch. Control measures including generation tripping or load shedding will be taken to prevent the system from transient instability.

c) 3rd Defense Line

The 3rd Defense Line consists of the out-of-step protection, controlled islanding, Under Frequency Load Shedding (UFLS) and Under Voltage Load Shedding (UVLS). It aims to limit the spread of cascading events by separating the whole power system into multiple islands which are controllable and self-sustainable. Firstly, the out-of-step is detected by the out-of-step protection, which launches the islanding. Then the system is partitioned into parts according to different constraints, the primary one of which is the GC. The stability of each island is finally achieved by UFLS and UVLS.

In the framework of the "Three Defense Lines", the GCI is related to online transient stability assessment in 2nd Defense Line and controlled islanding in 3rd Defense Line. Thus, the applications of GCI in power system stability assessment and control consist of the following two parts.

1.3.1 The application of GCI in transient stability assessment

The transient stability analysis of a power system, when subjected to a large disturbance, has always been an important issue. Extensive research activity has been pursued on solving this problem, resulting in various analysis approaches, among which the Extend Equal Area Criterion (EEAC) method[24, 25, 58] and the Single Machine Equivalent (SIME) method [27, 28, 59]play a significant role. These hybrid methods have a wide application in offline and online transient stability assessment because of their high accuracy and good adaptability. In these methods, all generators are first separated into two groups: the critical machines (CMs) group and the non-CMs (NMs) group. The dynamic performance of the multi-machine power system is then represented by the relative motion of two equivalent generators. An Equivalent Single-Machine Infinite Bus (E-SMIB) system is further presented to analyze the transient stability of the original system. For the application of E-SMIB based methods, the identification of CMs is of vital importance to the accuracy and validity of transient stability analysis[60]. Improper CM identification may lead to a delayed or even wrong transient stability detection result and invalid emergency control. A systematic method featuring rapid and accurate CM identification is thus necessary.

To realize the correct CM identification, two features of CMs must be taken into consideration. The first feature is that the CMs change with disturbances and operation conditions. Now that it is not practical to assume all possible disturbances and operations in advance by offline simulation, the CMs' identification should be based on online simulation or real-time measurement data. The second feature, although referred by only a few references, is that CMs may be variable during the whole dynamic process. It can be observed that some generators belong to the NMs group after the disturbance but change to the CMs group eventually, or vice versa. It is common in practical cases because continuous changes in system

conditions (i.e., multiple faults) occur in the power system[7]. To track the time evolution of CMs, a suggestion is made that the identification method is carried out in real-time.

Conventionally, CMs are identified by examining the relative swing curves between machines. However, it is computationally time-consuming to verify all possible combinations of generators because there are 2n-1 possible combinations for a system with machines. In [28], a significant reduction in combination numbers is realized by the sorted angles of generators. The machines are separated by the largest angle gap (LAG) between two adjacent machines at a short time after disturbance clearance. Although the conventional LAG method is independent of disturbances and system operations, the time of CM identification is difficult to choose, and the identification results are inaccurate in some cases. Moreover, the results of CM identification through this method are fixed for each case, and it cannot capture the change of CMs during the dynamic process.

On the other hand, it was found that the identification of CMs and NMs is similar to some extent to the issue of GCI. The generators in CMs (NMs) show similar behavior, but they have an obviously different dynamic performance than those in NMs (CMs), which is similar to the issue of GCI. One major difference is that the number of generator groups is fixed at two in CM identification, while it is not limited in coherency identification. Thus, the methods for coherency identification have the potential to identify CMs. Two kinds of methods, as discussed in section 1.2, are mainly reported in the references of coherency identification: model-based methods and measurement-based methods. Model-based methods neglect the effects of variable system operating conditions and configuration which can alter the system coherency. Thus, the coherent generators identified by model-based methods stay unchanged when subjected to different disturbances under different system conditions, which is apparently improper for CMs identification. The measurement-based methods can adapt to different disturbances and system conditions. However, they either need excessive computation, enormous training effort, or a wide time window. Moreover, the above-mentioned methods still fail to track the time evolution of CMs during the dynamic process.

In conclusion, a qualified CMs identification method must adapt to different operating conditions and disturbances, and be able to track the time evolution of CMs during the whole dynamic process. However, this problem has not still been well-addressed yet.

1.3.2 The application of GCI in controlled islanding

Controlled islanding is often regarded as the last control measure to protect the power system from severe blackouts. It aims to prevent the spread of cascading events by intentionally separating the grid into several self-sustainable islands.

Three critical issues need to be addressed regarding the controlled islanding: when to initiate the

islanding (the start-up criterion), where to separate the grid (the islanding strategy), and how to maintain the stability of islands after the separation (islands adjustment). To solve the first and third problems, different out-of-step protection schemes and islanding control methods were proposed in [61-69]. Different start-up criteria, in fact, result in different start-up times of the controlled islanding, which bring great challenges for the islanding strategy development. An effective islanding strategy scheme should be able to cooperate with different start-up criteria and develop a proper islanding strategy based on the system state at the startup time. Among all constraints in developing the islanding strategy, the generator coherency is the primary one to keep islands sustainable and stable[6]. Great efforts have been made to identify the generator coherency of the post-disturbance power system, as discussed in section 1.2.

The difficulty of the work of GCI for controlled islanding lies in three aspects. Firstly, it needs to track the variations of generator coherency accurately. The factors including different power flow mode, grid topology, disturbances and the moment of controlled islanding should be taken into account. Secondly, the GCI should be achieved rapidly at the moment that the controlled islanding starts. However, the start-up time of the CI is decided by out-of-step protection, which may differ with different protection principles. Thus, the GCI for CI is suggested to require less data, which increases the difficulty of the problem. Besides, to partition a power system, GCI is not the only problem to be solved. The coherency identification of non-generator buses, which is exactly the boundary of controlled islands, is rarely studied. Some of the mentioned methods may be suitable for GCI, but can not be extended to be used for grouping the non-generator buses.

In conclusion, a comprehensive GCI scheme for controlled islanding should not only be able to address the above-mentioned challenges of GCI but also can identify the coherency of non-generator buses. Besides, the scheme should use as less data as possible to coordinate with different out-of-step protections.

1.4 Contributions of this thesis

The main contributions of the thesis are:

a) **A novel concept of phase-plane trajectory vectors (PTV) is proposed to address the problems of dynamic generator coherency identification (GCI).** PTVs are computed efficiently with the aid of real-time measurement data from PMUs. Thus, it is self-adapted to the different system operating conditions and disturbances. Compared to conventional GCI method, the PTV based method provides abundant information about generator current and future state. As a result, the GCI based on PTV is accurate and fast. Besides, it can track the time-evolution of GC during the whole dynamic process. In addition, the computation is efficient and the application is flexible, which enhance its application in real-time scenarios.

b) **A PTV-based real-time CM identification scheme is proposed for power system transient stability assessment (TSA).** With the aid of the K-means clustering algorithm and PTVs, the scheme can identify CMs based on real-time measurement data. The dynamics of generators are well described by the feature matrix of PTVs, resulting in accurate and fast CMs identification. Besides, this scheme can adapt to different operating conditions and disturbances, and even track the time-evolution of CMs during the dynamic process. Compared with conventional CMs identification methods, the PTV based method also has advantages of faster computation, less information requirement, and higher accuracy, showing excellent potential for real-time application.

c) **A PTV based dynamic GCI scheme is proposed for controlled islanding.** This scheme can identify the dynamic generator coherency and make proper islanding strategy according to current system states. Firstly, the dynamics of generators are described by the PTVs on the PPG and the hierarchical clustering method is applied to determine the coherent groups. Then a PPB composed of bus voltage angle and frequency is built to assign the non-generator buses to the coherent groups. According to the identified coherent generators and areas, certain transmission lines are disconnected intentionally to form the separated islands. The advantages of the scheme is summarized as (i) it is self-adapted to different disturbances, topology changes, and various system conditions by using the real-time measurement data; (ii) it is simple and efficient because only two moments of data are required to determine the coherent generators and areas; (iii) it can identify the dynamic generator coherency according to the current system state so that it can cooperate with different start-up criteria of controlled islanding.

1.5 Outline of this thesis

The rest of the thesis is organized as follows.

In chapter 2, a profound analysis of the factors that influence GC is firstly made based on the rotor motion equations of generators. Then, the features of GC are summarized. Next, a novel concept of the Phase-plane trajectory Vector (PTV) is proposed to better describe the complex dynamics of generators and address the problems of GCI. Finally, the advantages and potentials of PTV based methods are summarized.

In chapter 3, a PTV based CMs identification scheme is proposed for TSA. The PTVs are firstly used to describe the dynamics of generators. Then the K-means clustering algorithm is applied to identify CMs based on the feature matrix of PTVs. Moreover, the validity of the CMs identification scheme is verified in the IEEE 39-bus 10-machine power system. Finally, the comparisons with other CMs identification methods made to highlight the advantages of PTV based method.

In chapter 4, a PTV based dynamic GCI scheme is proposed for controlled islanding. The PTVs are

firstly used to describe the dynamics of generators. Then the hierarchical clustering algorithm is applied to determine the coherency of generators based on the feature matrix of PTVs. Next, inspired by PTVs on the Phase Plane for Generators (PPG), a novel concept of phase plane for buses (PPB) is proposed and used to determine coherency of non-generator buses. The PTV based GCI scheme for controlled islanding is given finally and verified in the IEEE 39-bus 10-machine power system.

At the end of the thesis, Chapter 5 presents the conclusions and envisages some topics for future research.

2 Generator Coherency and Phase Trajectory Vector

After a disturbance occurs, the synchronous generators tend to behave in forms of multiple groups during the dynamic process. The transient responses of generators are similar in each group, and the phenomenon is called generator coherency (GC). The identification of GC is essential to power system stability assessment and control. Thus, the research on generator coherency identification has aroused widespread concern in the community.

To achieve accurate and fast generator coherency identification (GCI), the dynamic features of generators must be taken into consideration. Thus, in this chapter, a profound analysis of the factors that influence GC is firstly made based on the rotor motion equations of generators. Then, the features of GC are summarized. Next, a novel concept of the Phase-plane trajectory Vector (PTV) is proposed to describe the complex dynamics of generators. Finally, the excellent potential of PTV in GCI is verified in the IEEE 3-machine 9-bus power system.

2.1 Generator Coherency

2.1.1 Definition of GC

In fact, to the best of our knowledge, there is not an exact and straightforward definition of the generator coherency in current literature yet. Researchers tend to classify generators as coherent based on the similarity of swings curves of generator angles. However, the definition of similarity and the threshold value of coherency still haven't reached an agreement. A general definition of GC is given as:

Definition: Generator *i* and *j* are coherent during a period of $t \in [0, \tau]$ if their angles satisfy (2.1).

$$\max_{t\in[0,\tau]} \left| \Delta\delta_i(t) - \Delta\delta_j(t) \right| \le \varepsilon \tag{2.1}$$

where δ is the power angle of the generator and ε=5°~10°, $\tau = 1 \sim 3s$.

In [35], an updated and comprehensive review article of GC published recently, the definitions of GC are concluded as following two categories.

a) Type I: GC is defined based on the small-signal stability analysis of system models. This type of GC is independent to disturbances and used for generator aggregation in cases small disturbances occur.

b) Type II: GC is defined by tracking the dynamic response after disturbance occurrence without requiring any knowledge of system models. This type of GC differs under different disturbances and

operation condition. Thus, it can be used for transient stability assessment and control in cases large disturbances occur.

In this thesis, the definition of dynamic GC which belongs to type II is adopted. In the rest of the section, the features of GC during the whole dynamic process are concluded firstly, and then the factors that influence the dynamics of GC are studied.

2.1.2 Features of GC

As mentioned in the chapter of introduction, the features of GC are twofold: the variation due to different operating conditions and disturbances, and the time-evolution of GC during the dynamic process.

a) Variations of GC

It has been widely reported that the coherency of generators is different if the operating condition changes or the power system suffers from different disturbances. Two figures, Figure 2-1and Figure 2-2, are given below to illustrate the impacts of operating conditions and disturbances on GC.

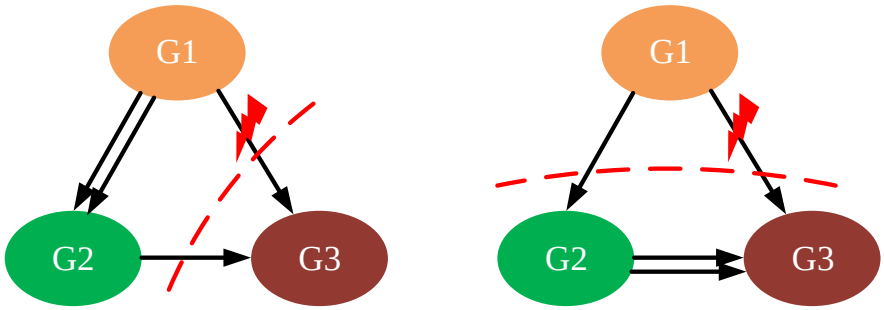

Scenario A: Operating Condition 1 Scenario B: Operating Condition 2

Figure 2-1 Variations of GC due to different operating operations

Figure 2-1 presents a schematic diagram of GC variations due to the changes in operating conditions. In this figure, G1, G2, and G3 are different generators or generator groups, and the arrows represent the electrical connections among generator groups. Two arrows indicate a strong connection while one arrow means a weak connection. The red symbol represents the disturbance and the red dashed line gives the result of generator coherency. In scenarios A and B, the disturbances are all the same, but the operating conditions are different. The operating operations, in fact, influence the electrical connections among generators before disturbances occur. In scenario A, the connection between G1 and G2 is much stronger than that between G2 and G3. As a result, after the disturbance occurs on the link between G1 and G3, G1 and G2 tend to form one coherent group while G3 belongs to an individual group. By contrast, the GC in scenario B is different. The connections between G2 and G3 is stronger than that between G1 and G3. Thus, G2 and G3 form one coherent group while G1 is alone.

Figure 2-2 presents a schematic diagram of GC variations due to the different disturbances. In

scenarios C and D, the operating conditions are all the same, but the disturbances are different. The disturbances, in fact, change the electrical connections among generators. Due to the same operating conditions, the electrical connections among generators are same in scenario C and D, as a result of which the connections between G1 and other two generators are stronger than that between G2 and G3. After the disturbance occurs on the link between G1 and G3 in scenario C, G1 and G2 tend to form one coherent group while G3 belongs to an individual group. By contrast, after the disturbance occurs on the link between G1 and G2 in scenario D, the GC changes to different results: G2 and G3 form one coherent group while G1 is alone.

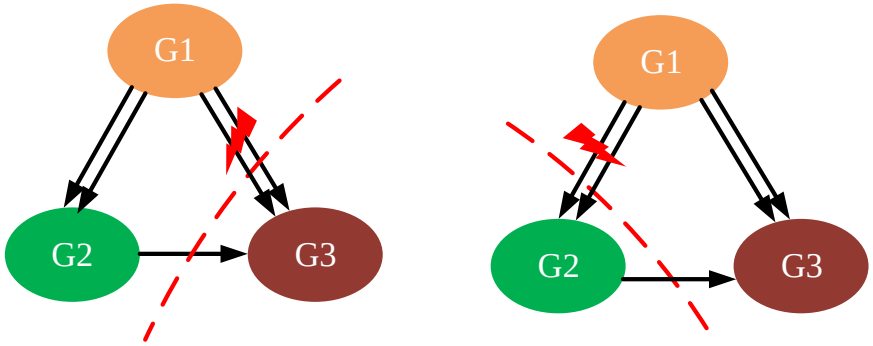

Scenario C: Disturbance 1 Scenario D: Disturbance 2

Figure 2-2 Variations of GC due to different disturbances

In conclusion, GC is different if the system is under different operating conditions or suffers from different disturbances.

b) Time-evolution of GC

Although referred by only a few references, GC may be time-varying during the whole dynamic process. It can be observed in certain cases that some generators belong to one coherent group after the disturbance but change to the different coherent groups eventually. This phenomenon of time-evolution of GC usually occurs in the multi-area interconnected power systems[1].

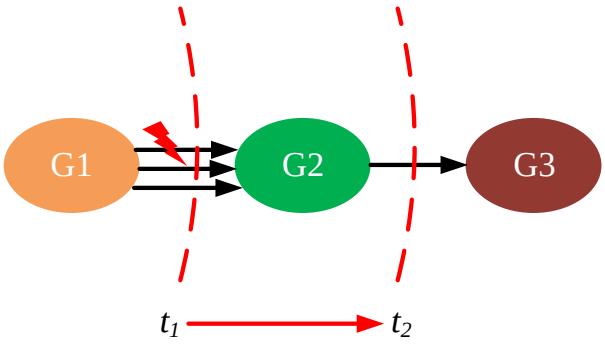

Figure 2-3 Time-evolution of GC during the dynamic process (Scenario E)

Figure 2-3 presents a schematic diagram of the GC time-evolution during the dynamic process. In scenario E, G2 has a strong electrical connection with G1 while has a relatively weak connection with G3. After the disturbance occurs on the link between G1 and G2, the results of GC detected at moment t_1 are {G1} and {G2, G3}. However, with time increasing, G2 tends to behave close to G1 due to the strong connection. The results of GC detected at moment t_2 change to {G1, G2}, and {G3}.

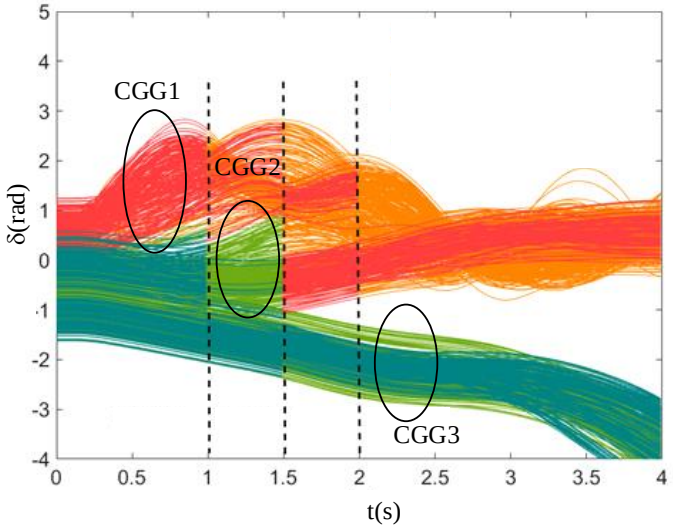

Figure 2-4 Time-evolution of GC in practical power system

Figure 2-4 gives an example of the time-evolution of GC in a practical power system. It presents the angle curves of 1526 generators. After the disturbance occurs, the oscillation begins between Coherent Generator Group (CGG)1 and {CGG2, CGG3}. With time increases, it changes to oscillate between {CGG1, CGG2} and {CGG3} eventually.

2.1.3 Impact factors of GC

To analyze the reason that GC has features of variation and time-evolution, the factors that greatly influence the dynamics of generators should be first studied. For better understanding, the analysis from the fundamental rotor motion equations is carried out.

For a multi-machine power system, the rotor motion equation of the *i*-th generator is

$$\begin{cases} \dfrac{d\delta_i}{dt} = \omega_0 \Delta\omega_i \\ M_{J,i}\dfrac{d\omega_i}{dt} = \Delta P_i = P_{m,i} - P_{e,i} - D\Delta\omega_i \end{cases}, i = 1, 2, \ldots, N \tag{2.2}$$

where δ_i, ω_0, $\Delta\omega_i$, ΔP_i, $P_{e,i}$ and $P_{m,i}$ are separately generator's synchronous angle, synchronous speed, angular speed deviation, unbalanced power, electric power, and mechanical power. N is the number of

generators. D is the damping factor and $M_{J,i}$ is the inertia moment.

According to the definition of GC in (2.1), the angles of coherent generators are close during the dynamic process. Thus, similar angle δ_i and angular speed $\Delta\omega_i$ of generators in each group are reasonable. It can be inferred from (2.2) that the factors of GC should consist of the following two variables.

(a) The inertia moment $M_{J,i}$

The inertia moment influences the GC results by affecting the angle oscillation period. Coherent generators tend to have similar oscillation period so that the angles remain close during the dynamic process. Thus the coherent generators should have similar inertia moment. Conversely, if the inertia moments are apparently different, the dynamic response of generators will show obvious differences.

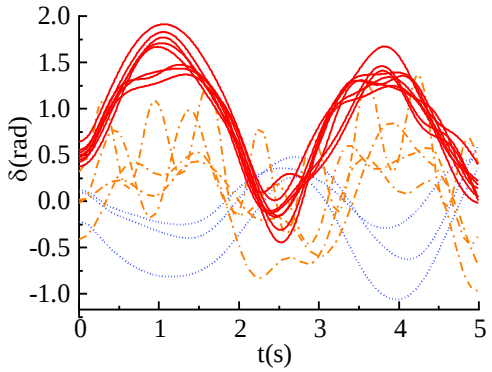

Figure 2-5 Generator incoherency caused by different inertia moments

Figure 2-5 gives an example of the impacts of inertia moments. Despite that the orange angle curves and the red angle curves have the same motion trend at first, they finally belong to different CGG due to their difference in swing periods which are greatly decided by the inertia.

(b) The unbalanced power ΔP_i

The role that unbalanced power plays to generators is like the motive force to a car. It drives the generators to increase or decrease the power angle. Thus, the symbol and value of unbalanced power decide the swing direction and amplitude of generators.

In conclusion, the dynamics of generators are influenced by factors including generators' inertia and unbalanced power. However, it is not feasible to determine GC based on these factors. For example, the unbalanced power is influenced by multiple factors such as the disturbances, operating conditions, and parameters of generators, making it impossible to be measured directly. Thus, a method that taking account of dynamic features of generators and being achieved based on measurement data is necessarily required for GCI.

2.2 Phase-plane Trajectory Vector

To identify the dynamic GC, a novel concept of Phase-plane Trajectory Vector (PTV) is proposed in this section. The definition and features are discussed as follows.

2.2.1 Definition of PTV

According to the definition of GC in (2.1), the dynamics of generators which is described by angles δ_i and speed $\Delta\omega_i$ in (2.2) should be taken into consideration. Conventional GCI methods focus on the angle or angular speed separately. In this regard, the technology of phase plane provides a profound view for this issue because both angle and angular speed of generators can be studied at the same time. Inspired by this technology, a novel concept of PTV is proposed to describe the dynamics of generators during the transient process.

The phase plane constructed by the angle δ_i and the angular speed $\Delta\omega_i$ describes the state of the generator, which are influenced by regulators such as AVR, governor and PSS. The dynamic performance of a generator can be visible on the phase plane, and each phase point $\left(\delta_i(t), \Delta\omega_i(t)\right)$ represents the state of the *i*-th generator at time *t*.

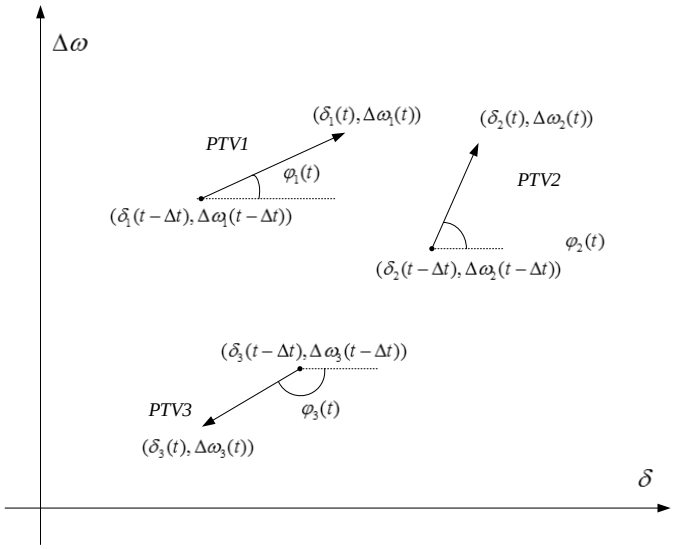

Figure 2-6 PTVs on the phase plane

The PTV is defined as the vector from point $\left(\delta_i(t-\Delta t), \Delta\omega_i(t-\Delta t)\right)$ to the point $\left(\delta_i(t), \Delta\omega_i(t)\right)$ on the phase plane, representing the motion the *i*-th generator. Δt is the time interval of measurement data. From (2.2), only two sample points are necessary to obtain the PTV of the *i*-th generator, each of which includes the information of generators' angle and angular speed deviation. For a power system with *N* generators, the number of PTVs obtained at each moment is *N*. Figure 2-6 shows the PTVs on the phase

plane, by which it is clear to identify the differences among different generators.

2.2.2 Features of PTV

Figure 2-6 shows that each PTV can be uniquely determined by the location and direction.

PTV location. The location of PTV indicates the angle and angular speed deviation of generators, which are important for CMs identification. The location of generators is available by

$$[\boldsymbol{\delta} \quad \boldsymbol{\Delta\omega}] = \begin{bmatrix} \delta_1(t) & \Delta\omega_1(t) \\ \delta_2(t) & \Delta\omega_2(t) \\ \vdots & \vdots \\ \delta_N(t) & \Delta\omega_N(t) \end{bmatrix} \tag{2.3}$$

PTV angle. The angles of PTVs relative to the positive x-axis represent the motion trend of generators. Taking motion trend into consideration can make the CMs identification faster and more accurate. The feature of PTVs angles can be obtained by(2.4):

$$\boldsymbol{\varphi} = \begin{bmatrix} \varphi_1(t) & \varphi_2(t) & \cdots & \varphi_N(t) \end{bmatrix}^T \tag{2.4}$$

The motion angle of each PTV is computed by(2.5):

$$\varphi_i(t) = \arccos\left(\frac{\vec{p}_i \vec{e}}{|\vec{p}_i||\vec{e}|}\right) \tag{2.5}$$

where $\vec{p}_i = (\delta_i(t) - \delta_i(t-\Delta t), \Delta\omega_i(t) - \Delta\omega_i(t-\Delta t)), \vec{e} = (1,0)$. From(2.5), the value range of the PTV angle is $(0, \pi)$.

The feature matrix of PTVs is thus obtained as

$$\mathbf{A} = [\boldsymbol{\delta} \quad \boldsymbol{\Delta\omega} \quad \boldsymbol{\varphi}] = = \begin{bmatrix} \delta_1(t) & \Delta\omega_1(t) & \varphi_1(t) \\ \delta_2(t) & \Delta\omega_2(t) & \varphi_2(t) \\ \vdots & \vdots & \vdots \\ \delta_N(t) & \Delta\omega_N(t) & \varphi_N(t) \end{bmatrix} \tag{2.6}.$$

The standardization of the feature matrix is further applied to balance the weight of three variables as follows.

$$\mathbf{A}_s(t) = \begin{bmatrix} \vec{V}_{1s} \\ \vec{V}_{2s} \\ \vdots \\ \vec{V}_{Ns} \end{bmatrix} = \begin{bmatrix} \delta_{1s}(t) & \Delta\omega_{1s}(t) & \varphi_{1s}(t) \\ \delta_{2s}(t) & \Delta\omega_{2s}(t) & \varphi_{2s}(t) \\ \vdots & \vdots & \vdots \\ \delta_{Ns}(t) & \Delta\omega_{Ns}(t) & \varphi_{Ns}(t) \end{bmatrix} \tag{2.7}$$

In(2.7), $\delta_{is}(t) = \dfrac{\delta_i(t)}{\sum \delta_i(t)/N}, \Delta\omega_{is}(t) = \dfrac{\Delta\omega_i(t)}{\sum \Delta\omega_i(t)/N}, \varphi_{is}(t) = \dfrac{\varphi_i(t)}{\pi}$.

The PTV angle is variable during the dynamic process, as shown in Figure 2-7. It shows the motion of the PTV of one generator when subjected to a large disturbance. The clockwise moving PTV indicates that the generator leaves the stable operating point and moves towards the new stable equilibrium point (SEP). Table 2-1 shows the value of φ_i is corresponding to the generator state. When the PTV locates in upper half part of the phase plane, the generator swings forward, during which the value of φ_i is in range of $(0, \pi/2)$. And if the PTV locates in the lower half part of the phase plane, the generator swings back and the value of φ_i is in range of $(\pi/2, \pi)$.

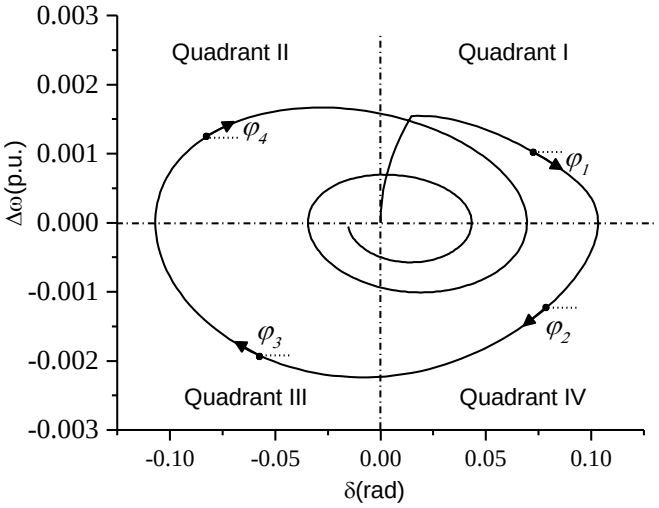

Figure 2-7 The motion of PTV on the phase plane

Table 2-1 The PTV angle and Generator state

PTV angle	Quadrant	Range	Generator State
φ_1	I ($\delta > 0, \Delta\omega > 0$)	$(0, \pi/2)$	Swing forward
φ_2	VI ($\delta > 0, \Delta\omega < 0$)	$(\pi/2, \pi)$	Swing back
φ_3	III ($\delta < 0, \Delta\omega < 0$)	$(\pi/2, \pi)$	Swing back
φ_4	II ($\delta < 0, \Delta\omega > 0$)	$(0, \pi/2)$	Swing forward

2.2.3 Advantages of PTV

For coherent generators, the power angle increments should be similar over time. As a result, not only the angle but also the future motion of coherent generators should be similar during the given specific period. In other words, the PTVs should be similar at any time during this period if these generators are coherent. Thus, the PTVs at time *t* can be applied to identify coherent generators for the near period.

Compared with conventional GCI methods, the proposed concept of PTV has advantages in describing the dynamics of generators as follows.

a) Model-free

It can be inferred that, from the definition of PTVs and the feature matrix computation in (2.7), the PTV based GCI method belongs to the model-free category. All required information to compute PTVs is the angle δ_i and speed $\Delta\omega_i$ of generators, which can be obtained from PMUs in real-time. Thus, the PTV based GCI method has the same advantages as other measurement-based methods. For example, no mode related information including the power flow, grid topology, and generator modes is required to obtain PTVs. Besides, PTV based GCI method adapts to different operating conditions and disturbances, which greatly enhance its application.

b) Abundant information

The PTVs provide abundant information about generator dynamics, which is far more than conventional methods. PTVs not only focus on the angle but also pay attention to the angular speed and motion trend. In other words, PTVs can describe the current state as well as predict the future motion of generators by(2.4). Figure 2-8 presents the time-domain generator angle curves for comparison with the PTVs on phase-plane in Figure 2-7. In the time-domain curves, it takes a period of time to identify the current state of generators. By contrast, one PTV computed by two sample points can clearly describe the quadrant it locates and the directions it moves next moment. This feature significantly improves the accuracy and identification speed of GCI. Moreover, the features of PTV are visible and easy to accept for humans, which may benefit its application in power system real-time dispatch.

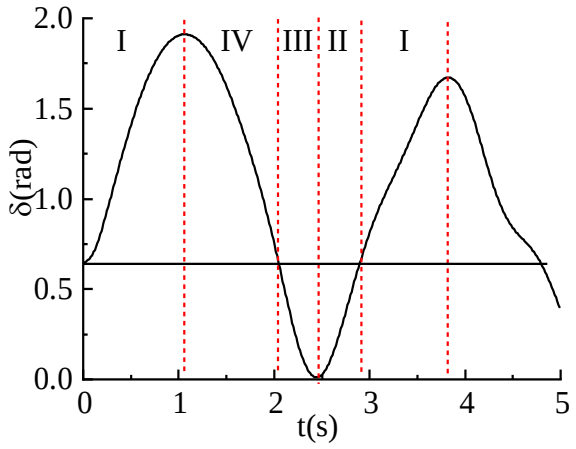

Figure 2-8 The time-domain curves of generator angle

c) Dynamic GC trace

One of the greatest advantages of the PTV based GCI method is that it can track the time-evolution of GC. It is achieved by an updated-to-time feature matrix $\mathbf{A_s(t)}$. It can be inferred from (2.7) that the feature matrix is only related to the current state of generators, neglecting the effects of historical data.

And the matrix keeps updating with real-time measurement data from PMUs. Once the GC changes during the dynamic process, the feature matrix can reflect the changes and ensure the results of GCI updated.

d) Flexible application

The calculation of the feature matrix $\mathbf{A_s(t)}$ only requires two moments of sample data, and the computation can be achieved at each moment. It means the results of GCI can be given at any moments as long as measurement data provided. It is a huge improvement in research of GCI, which extends the application of GCI in power system stability assessment and control. For example, the PTV based GCI methods can offer reliable GCI results at whatever start-up time of controlled islanding control.

e) Efficient computation

The computation of the PTV feature matrix in (2.6) is simple and efficient. This advantage of PTV based method will enhance its application in real-time scenarios.

2.3 Summary

In this chapter, the definition of GC is first clarified. Then the features of GC during the dynamic process are concluded as twofold: 1) the variation of GC to different operating conditions and disturbances, and 2) the time-evolution of GC Based on the fundamental rotor motion equations, analysis of the factors that greatly influence the generator dynamics is studied in this chapter.

Based on the above analysis, a novel concept of PTV is proposed to address the problems of GCI. we first give a clear definition of PTVs and then extracts the features of PTVs. The advantages of the proposed PTVs are finally summarized into 5 aspects which includes adapting to different operating conditions and disturbances, providing abundant information for accurate and fast GCI, being able to tack the time-evolution of GC, flexible application and the efficient computation.

In conclusion, the proposed PTVs can address the problems of dynamic generator coherency identification and has excellent potential for real-time applications.

3 PTV Based Real-Time CMs Identification Scheme for TSA

The transient stability assessment (TSA) of a power system, when subjected to a large disturbance, has always been an important issue. Extensive research activity has been pursued on solving this problem, resulting in various analysis approaches, among which the Equivalent Single-Machine Infinite Bus (E-SMIB) based TSA methods play a significant role. In these methods, all generators are separated into two groups: the critical machines (CMs) group and the non-CMs (NMs) group. The identification of CMs is of vital importance to the accuracy and validity of transient stability analysis. A systematic method featuring rapid and accurate CM identification is thus necessary.

To realize the correct CM identification, two features of CMs must be taken into consideration. The first feature is that the CMs change with disturbances and operation conditions. The second feature is that CMs may be variable during the whole dynamic process. In fact, the identification of CMs is similar to some extent to the issue of GCI: generators that belong to CMs or NMs are usually coherent. The only difference is that the number of generator groups is fixed at two in CM identification, while it is not limited in coherency identification. Thus, the PTV based GCI method proposed in chapter 2 has the potential to be applied to the real-time CMs identification for TSA.

In this chapter, a PTV based CMs identification scheme is proposed for TSA. The PTVs are firstly used to describe the dynamics of generators. Then the K-means clustering algorithm is applied to identify CMs based on the feature matrix of PTVs. Moreover, the validity of the CMs identification scheme is verified in the IEEE 39-bus 10-machine power system. Finally, the comparisons with other CMs identification methods made to highlight the advantages of PTV based method.

3.1 Critical Machines and Non-critical Machines

Following the definition of PTVs in chapter 2, the feature matrix of PTVs $\mathbf{A}$ is obtained in(2.6). The matrix $\mathbf{A}$ represents the features of PTVs, by which generators can be divided into two groups: CMs and NMs. Different from other CMs identification methods, the proposed method not only focus on the angle but also pay attention to the angular speed and motion trend, which indicates the future motion of generators by(2.5). Thus, the proposed PTVs describe much more information than the angle curves of generators. It is also noted that $\mathbf{A}$ is time-varying, which is computed with PMU information at each moment. By the real-time updated feature matrix, PTVs describe the dynamic performance of generators visibly. The time-evolution of CMs can thus be tracked by PTVs.

3.2 Centre Of Inertia (COI) processing of measurement data

First of all, the relative motion among generators attracts more attention to CMs identification. The Centre Of Inertia (COI) processing is necessary to analyze the relative dynamic performance of generators [20]. The angle and angular velocity deviation of the COI are defined as

$$\delta_{COI}(t)=\frac{\sum_{i=1}^{N}M_{J,i}\delta_i(t)}{\sum_{i=1}^{N}M_{J,i}},\Delta\omega_{COI}(t)=\frac{\sum_{i=1}^{N}M_{J,i}\Delta\omega_i(t)}{\sum_{i=1}^{N}M_{J,i}} \tag{3.1}$$

It is noted that the COI is time-varying which is decided by state variables. Thus, the motion of each generator relative to the COI is obtained by

$$\theta_i(t)=\delta_i(t)-\delta_{COI}(t),\Delta\tilde{\omega}_i(t)=\Delta\omega_i(t)-\Delta\omega_{COI}(t) \tag{3.2}$$

3.3 PTV based real-time identification of CMs

To identify the CMs and NMs, the K-means clustering method is applied. The K-means clustering method is popular for cluster analysis in data mining. It has the advantages of little computation, fast clustering, and high accuracy. The difficulty of the K-means clustering method is to determine the K number of coherent groups. However, K is fixed to 2 in the special scenario of CMs identification. Following simulations also verify the applicability of K-means clustering.

The details of the K-means method can be available from the literature [16]. Firstly, two clustering centers are given at the beginning as: $c_1:(\theta_{c1},\Delta\tilde{\omega}_{c1},\tilde{\varphi}_{c1})$ and $c_2:(\theta_{c2},\Delta\tilde{\omega}_{c2},\tilde{\varphi}_{c2})$. For a fast calculation, the initial centers are selected as the generator with the largest angle and the one with the least angle. Then the distance from generators to each clustering center is computed with the feature matrix. To balance the impact of each feature on distance computation, the units for $\theta_i(t),\Delta\tilde{\omega}_i(t)$ and $\tilde{\varphi}_i(t)$ are *rad*, *p.u.* and rad/π. The new feature matrix of PTVs at each moment is:

$$\tilde{\mathbf{A}}=[\boldsymbol{\theta}\quad\Delta\tilde{\boldsymbol{\omega}}\quad\tilde{\boldsymbol{\varphi}}]=[\boldsymbol{\theta}\quad\Delta\tilde{\boldsymbol{\omega}}\quad\boldsymbol{\varphi}/\pi] \tag{3.3}$$

The Euclidean distance is used to measure the distance of *i*-th generators to the two cluster centers:

$$\begin{aligned}dis(i,c_1)&=\sqrt{(\theta_i-\theta_{c1})^2+(\Delta\tilde{\omega}_i-\Delta\tilde{\omega}_{c1})^2+(\tilde{\varphi}_i-\tilde{\varphi}_{c1})^2}\\dis(i,c_2)&=\sqrt{(\theta_i-\theta_{c2})^2+(\Delta\tilde{\omega}_i-\Delta\tilde{\omega}_{c2})^2+(\tilde{\varphi}_i-\tilde{\varphi}_{c2})^2}\end{aligned} \tag{3.4}$$

Generators are assigned to the group of closer clustering center. For example, the *i*-th generator belongs to the group C_1 if $dis(i,c_1)<dis(i,c_2)$. By this way, generators are divided into two groups. New

clustering centers are obtained by these two groups:

$$\begin{aligned} c_{1,new} &: (\frac{\sum \theta_i}{m}, \frac{\sum \Delta\tilde{\omega}_i}{m}, \frac{\sum \tilde{\varphi}_i}{m}), i \in \text{Group}(c_1) \\ c_{2,new} &: (\frac{\sum \theta_j}{n}, \frac{\sum \Delta\tilde{\omega}_j}{n}, \frac{\sum \tilde{\varphi}_j}{n}),\ j \in \text{Group}(c_2), \text{ and } m+n=N \end{aligned} \tag{3.5},$$

where m and n are separately the number of generators in Group(C1) and Group(C2). New distances are computed and the cycle process continues until the clustering result remains unchanged. The group with larger inertia is usually regarded as the CMs and the rest group is NMs.

The overall procedure for real-time CMs identification can be summarized in the following steps:

step 1. Read real-time information from PMUs which includes the angle, angular speed deviation of generators of current moment;

step 2. Make the COI processing of original information and initialize the data by subtracting the stable operation state information;

step 3. Check whether generators are out-of-step by angle threshold (i.e. 2π). If the angle of the generator is larger than the threshold, this generator is marked as an out-of-step generator;

step 4. Obtain the feature matrix $\tilde{\mathbf{A}}$ of rest generators at moment *t* by (3.3);

step 5. Apply the K-means clustering method based on the feature matrix $\tilde{\mathbf{A}}$ and output the CMs identification results;

step 6. Return to step 1 and keep tracking the change of CMs until the system runs to a new stable operating point.

3.4 Case study

In this section, the proposed PTV based method for CMs identification is tested in the New England 39 bus 10 machines power system as shown in Figure 3-1. The generators of the tested power system adopt the two-axis generator model equipped with AVRs and PSSs[70]. The dynamic of the system is simulated on the PSASP- a platform for transient simulation and analysis. The time interval of output data is 10ms, which is regarded as the PMU information in the real-time CMs identification scheme. Many cases have been simulated, however, only three typical cases are presented here to show the validity of the proposed method.

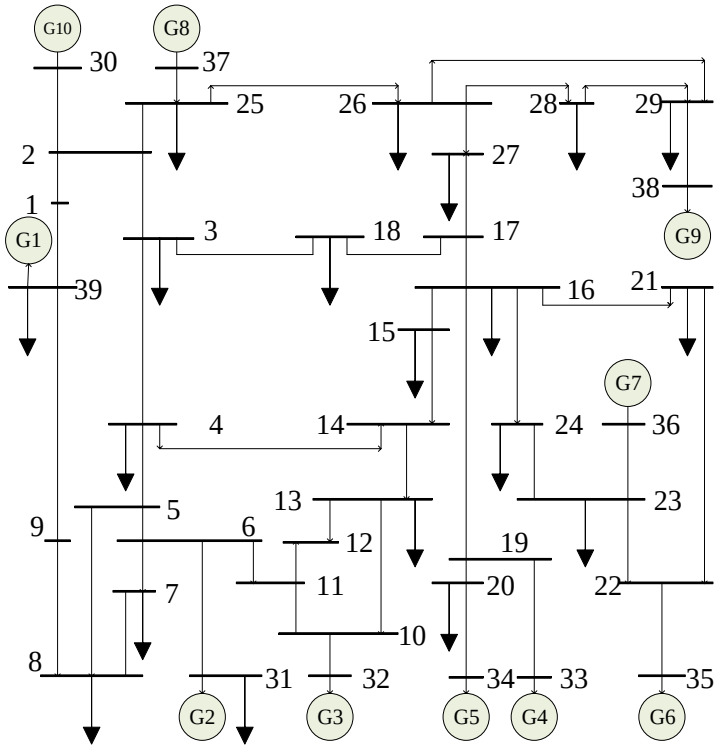

Figure 3-1 New England 39-bus 10-machine power system

3.4.1 Case 1

In case 1, a three-phase short circuit ground fault occurs in the middle of transmission line 21-22 at 0s, and then the fault line is eliminated at 0.1s. The system is transient stable eventually and the angle curves of generators are shown in Figure 3-2. The CMs identification results are shown in Figure 3-3.

In Figure 3-2, the groups to which each generator belongs are distinguished by different colors. The Blue blocks stand for the CMs while the Red blocks stand for the NMs. From Figure 3-3, there is only one mode of CMs and NMs during the whole dynamic process: group {G1} and group {G2-G10}. Figure 3-2 also shows the figures of PTVs at different moments such as 0.6s, 1s and 2s. These moments are selected because either angles or angular speed deviation are similar and misidentification is easy to obtain by other CMs identification methods (which will be further discussed in section 3.4). However, the figures of PTVs show obvious differences in the locations or the motion trend between CMs and NMs. The initial state in Figure 3-2 is the (0,0) in the phase plane, standing for the stable operation point of generators before the disturbance. The feature matrix $\tilde{\mathbf{A}}$ of these moments is presented in Table 3-1. During the whole dynamic process, the CMs and NMs identification result keeps unchanged: the CMs are {G2-G10} and NM is {G1}, which is identical to the above analysis. The excellent performance of the PTV method in case 1 benefits from the typical features selected which well describes the dynamic behavior of generators.

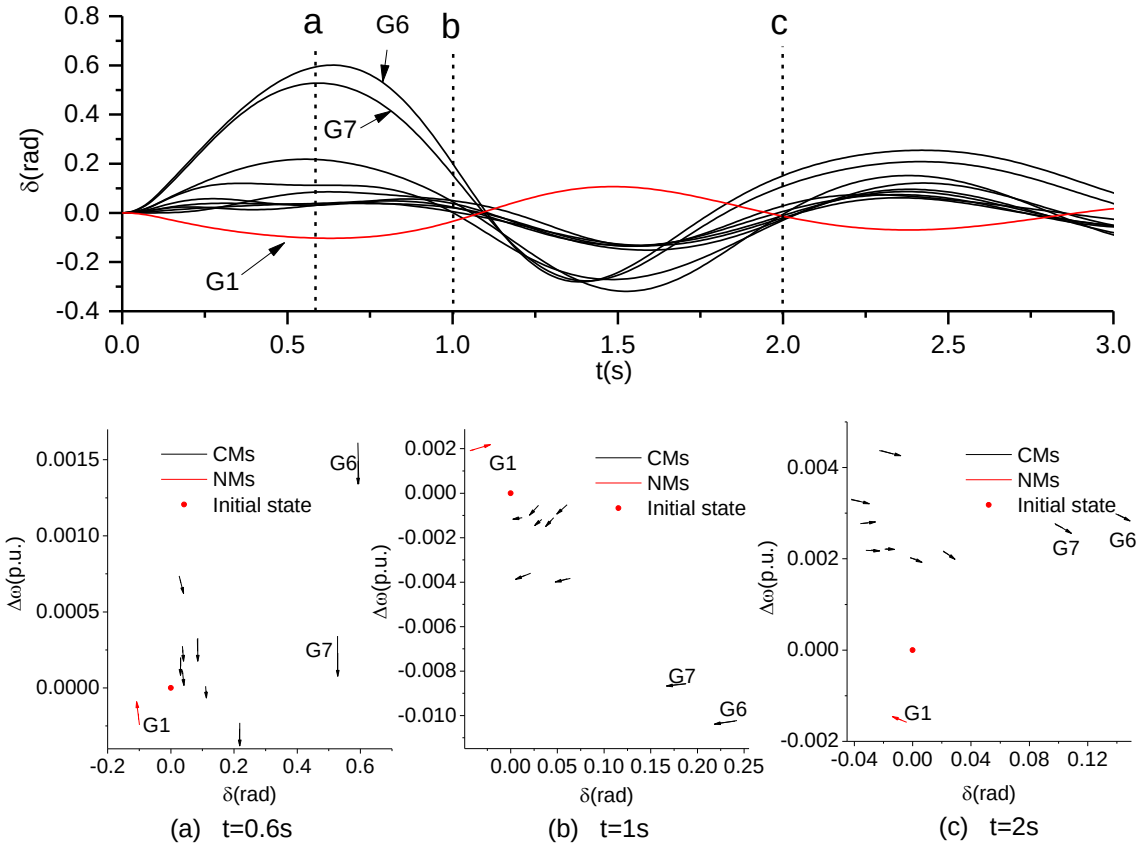

Figure 3-2 Generator angle curves and the PTVs at different moments in Case 1

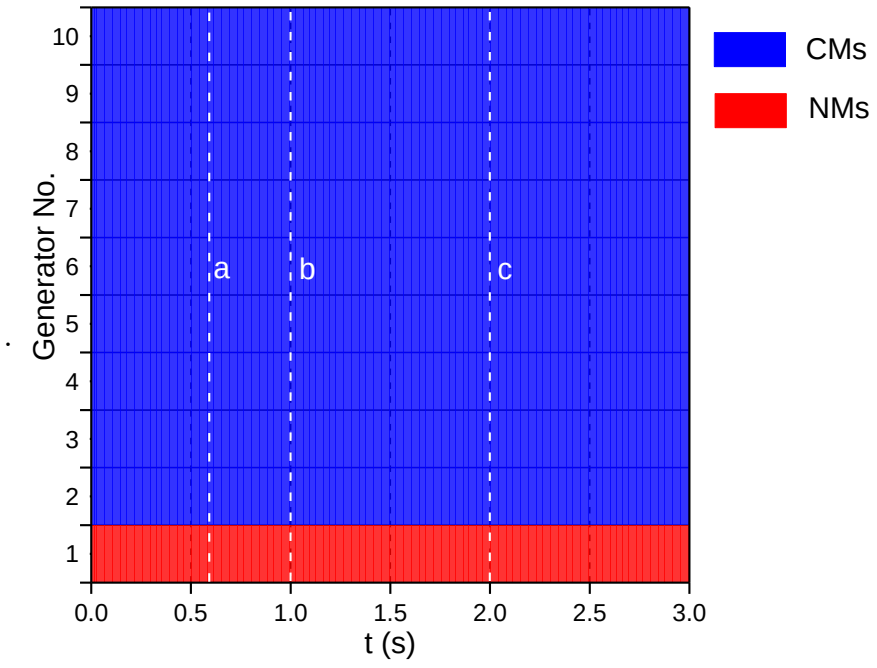

Figure 3-3 The CMs identification results in Case 1

Table 3-1 Feature Matrix at different times and CMs identification results in Case 1

Time	t=0.6s			t=1s			t=2s		
Gen. No.	$\boldsymbol{\theta}$	$\boldsymbol{\Delta\tilde{\omega}}$	$\tilde{\varphi}$	$\boldsymbol{\theta}$	$\boldsymbol{\Delta\tilde{\omega}}$	$\tilde{\varphi}$	$\boldsymbol{\theta}$	$\boldsymbol{\Delta\tilde{\omega}}$	$\tilde{\varphi}$
G1	-0.10255	-0.00017	0.96455	-0.03834	0.00197	0.00377	-0.01062	-0.00150	0.99727
G2	0.03758	0.00009	0.01884	0.02233	-0.00086	0.98856	0.00205	0.00199	0.00300
G3	0.03801	0.00025	0.01373	0.02600	-0.00141	0.98935	-0.01506	0.00221	0.00042
G4	0.11224	-0.00002	0.03777	0.00877	-0.00380	0.99475	-0.03588	0.00326	0.00183
G5	0.21709	-0.00037	0.04697	0.05333	-0.00393	0.99625	-0.01348	0.00430	0.00294
G6	0.59500	0.00134	0.03086	0.22092	-0.01035	0.99825	0.14600	0.00289	0.00493
G7	0.52779	0.00009	0.17853	0.17180	-0.00863	0.99850	0.10283	0.00268	0.00470
G8	0.03150	0.00069	0.00493	0.00711	-0.00114	0.99754	-0.02430	0.00218	0.00120
G9	0.03124	0.00020	0.05906	0.04095	-0.00133	0.98600	-0.03064	0.00279	0.00088
G10	0.08475	0.00024	0.04807	0.05145	-0.00084	0.99253	0.02492	0.00209	0.00600
Identification Result	CMs: G2-G10			CMs: G2-G10			CMs: G2-G10		
	NMs: G1			NMs: G1			NMs: G1		

3.4.2 Case 2

In case 2, same three-phase short circuit ground fault occurs on the transmission line 21-22 at 0s, and the fault line is eliminated at 0.2s. Due to the delayed relay operation, the system is unstable eventually and the angle curves of generators are shown in Figure 3-4. The CMs identification results are shown in Figure 3-5.

In Figure 3-5, generator groups are distinguished by different colors. The blue blocks stand for the CMs while the red blocks stand for the NMs. These out-of-step generators are especially represented by black blocks. The time-evolution of generator groups are clearly observed in Figure 3-5. G1 is the NM and rest generators are CMs at first after the fault clearance in the period of 0-0.66s. G6 and G7 become CMs later in the period of 0.67s-1.58s. The angles of G6 and G7 increase continuously and become out-of-step after 1.59s. Then G5 is identified as CM in the period of 1.59s-2.21s. After 2.22s, G5 become out-of-step and G4 is identified as CM. This time-evolution of CMs often occurs in transient unstable cases. Influenced by unstable machines, some machines in NMs change to the CMs and become out-of-step eventually. Conventional methods fail to identify the changes of CMs in such cases. However, the time-evolution of CMs are tracked successfully by the proposed PTV method thanks to its ability of real-time identification. As it is shown in Figure 3-4, different CMs are identified by the PTVs at different moments. The feature matrices and identification results are summarized in Table 3-2.

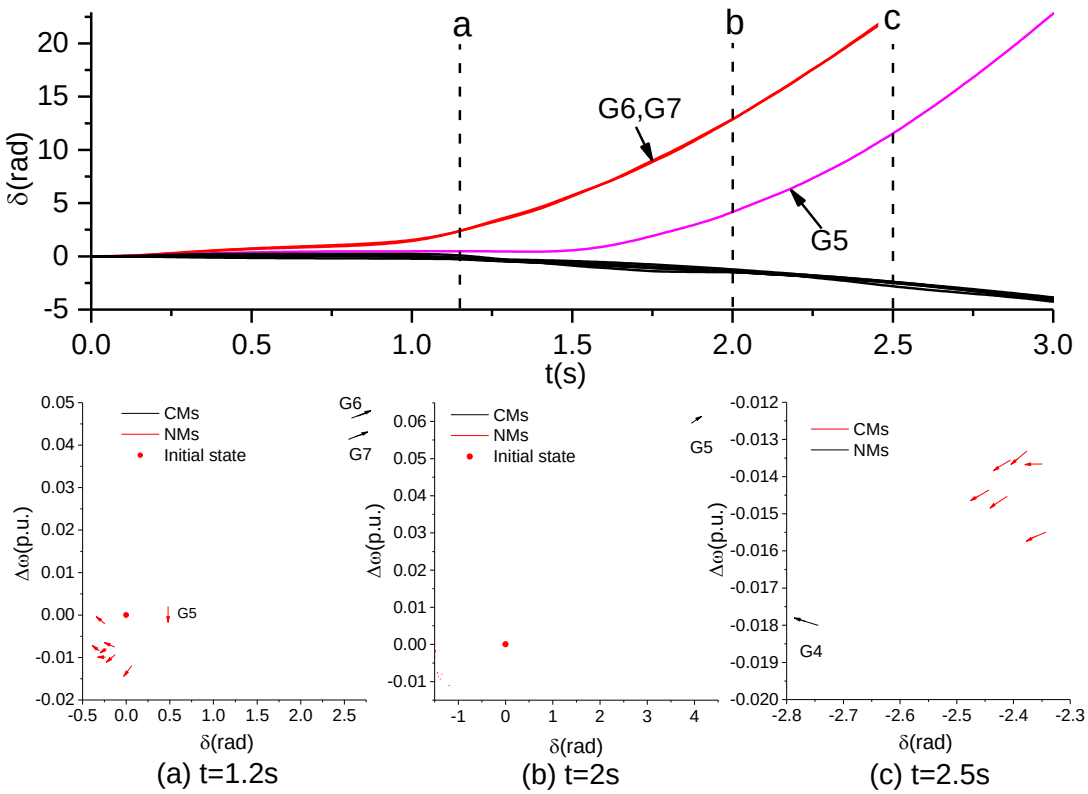

Figure 3-4 Generator angle curves and the PTVs at different moments in Case 2

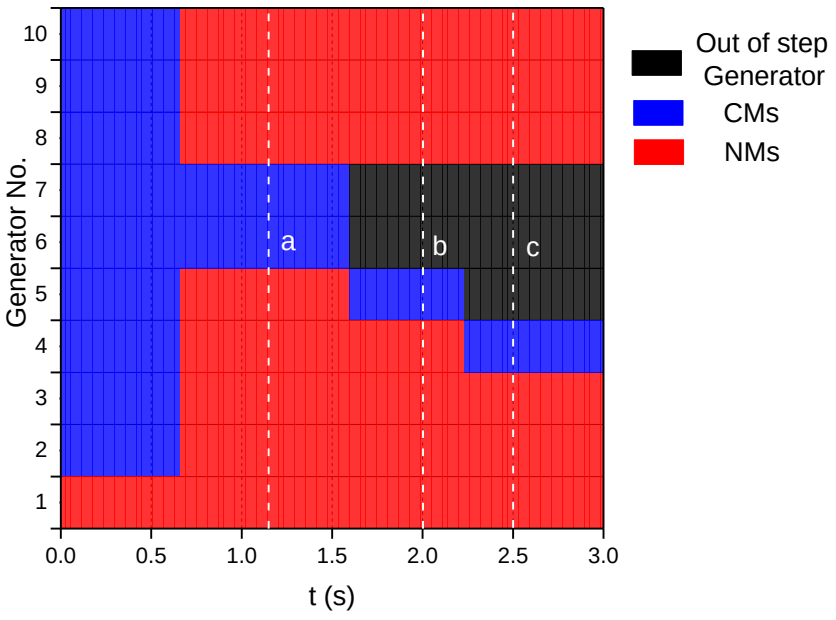

Figure 3-5 The CM identification results in Case 2

Table 3-2 Feature Matrix at different times and CMs identification results in Case 2

Time	t=1s			t=2s			t=2.5s		
Gen. No.	$\boldsymbol{\theta}$	$\boldsymbol{\Delta\tilde{\omega}}$	$\tilde{\varphi}$	$\boldsymbol{\theta}$	$\boldsymbol{\Delta\tilde{\omega}}$	$\tilde{\varphi}$	$\boldsymbol{\theta}$	$\boldsymbol{\Delta\tilde{\omega}}$	$\tilde{\varphi}$
G1	-0.1025	-0.00017	0.96455	-1.20475	-0.01113	0.997498343	-2.37493	-0.01366	0.9999
G2	0.0375	0.00009	0.01884	-1.39163	-0.00937	0.997574444	-2.43081	-0.01378	0.9971
G3	0.03801	0.00025	0.01373	-1.42900	-0.00860	0.999138786	-2.43873	-0.01480	0.99688
G4	0.11224	-0.00002	0.03777	-1.48788	-0.00214	0.939128812	-2.77802	-0.01784	0.9984
G5	0.21709	-0.00037	0.04697	4.04855	0.06060	0.003082456	-	-	-
G6	0.59500	0.00134	0.03086	-	-	-	-	-	-
G7	0.52779	0.00009	0.17853	-	-	-	-	-	-
G8	0.03150	0.00069	0.00493	-1.4425	-0.00763	0.996791332	-2.47063	-0.01460	0.99719
G9	0.03124	0.00020	0.05906	-1.45613	-0.00778	0.99948356	-2.40175	-0.01363	0.99598
G10	0.08475	0.00024	0.04807	-1.35483	-0.00804	0.997597503	-2.37230	-0.01568	0.99793
Identification Result	Out of Step Generators: None			Out of Step Generators: G6, G7			Out of Step Generators: G5-G7		
	CMs: G6-G7			CMs: G5			CMs: G4		
	NMs: G1-G5, G8-G10			NMs: G1-G4, G8-G10			NMs: G1-G3, G8-G10		

3.4.3 Case 3

Two continuous disturbances are simulated in the case 3. The first three-phase short circuit ground fault occurs on the line 21-22 at 0s, and then the fault line is eliminated at 0.1s. Afterward, the second three-phase short circuit ground fault occurs on line 28-29 at 2s, and then the fault line is eliminated at 2.1s. The angle curves of generators and PTVs at different times are shown in Figure 3-6 and CMs identification results are given in Figure 3-7.

Before the occurrence of the second disturbance, CMs in case 3 are same as that in case 1. However, the second disturbance changes the stability of the power system and influences the mode of CMs and NMs. G9 begins to accelerate and becomes unstable eventually. Figure 3-7 shows the evolution of CMs in Case 3. CMs are {G2-G10} in period of 0-2.4s and change to {G9} in period of 2.41s-3s. The feature matrix and identification results of different moments are presented in Table 3-3. The changes of CMs are identified correctly via the proposed method.

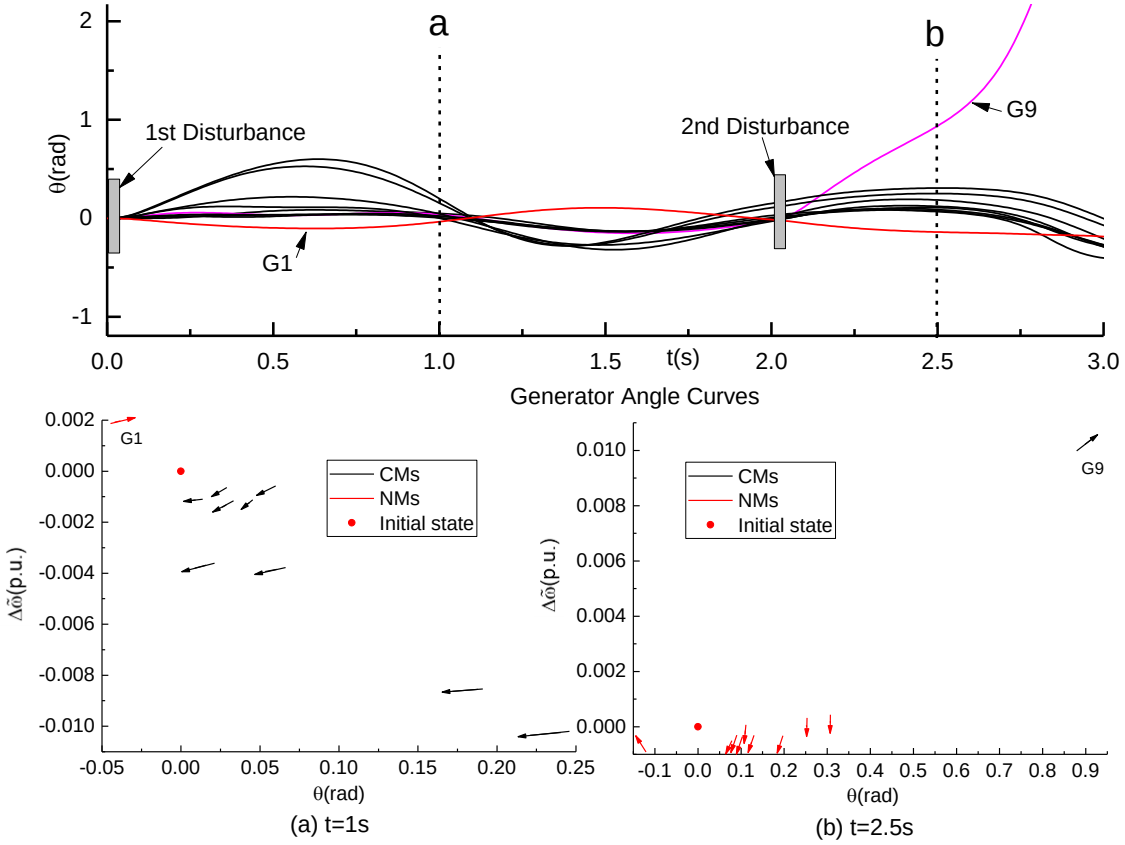

Figure 3-6 Generator angle curves and the PTVs at different moments in Case 3

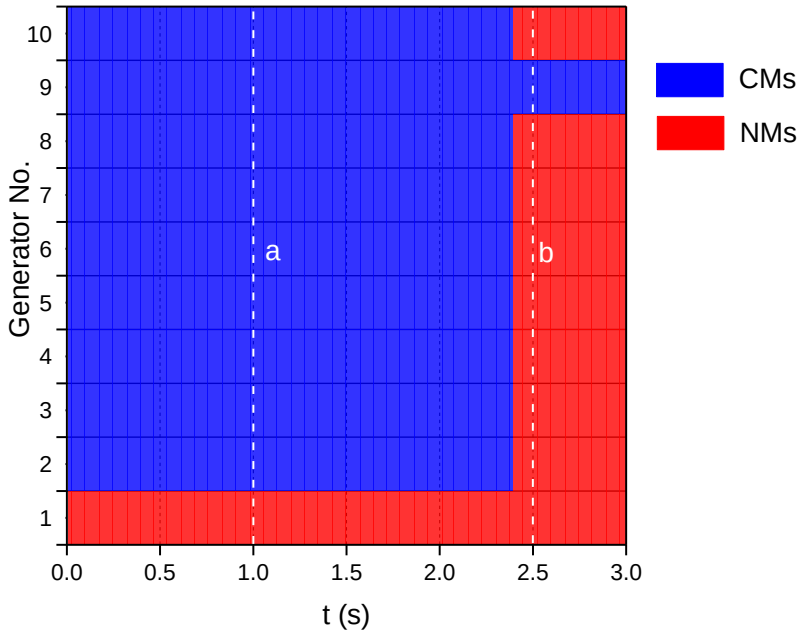

Figure 3-7 The CM identification results in Case 3

Table 3-3 Feature Matrix at different times and CMs identification results in Case 3

Time	t=1s			t=2.5s		
Gen. No.	θ	$\Delta\tilde{\omega}$	$\tilde{\varphi}$	θ	$\Delta\tilde{\omega}$	$\tilde{\varphi}$
G1	-0.03834	0.00197	0.00377	-0.13840	-0.00047	0.99144
G2	0.02233	-0.00086	0.98856	0.07721	-0.00088	0.98272
G3	0.02600	-0.00141	0.98935	0.09052	-0.00095	0.98402
G4	0.00877	-0.00380	0.99475	0.12316	-0.00063	0.97833
G5	0.05332	-0.00393	0.99625	0.18755	-0.00080	0.97853
G6	0.22091	-0.01035	0.99825	0.30742	-0.00014	0.96302
G7	0.17180	-0.00863	0.99850	0.25197	-0.00001	0.91282
G8	0.00711	-0.00114	0.99754	0.06945	-0.00085	0.99071
G9	0.04094	-0.00133	0.98600	0.91754	0.01045	0.00383
G10	0.05145	-0.00084	0.99253	0.10929	-0.00026	0.90549
Identification Result	CMs: G2-G10			CMs: G9		
	NMs: G1			NMs: G1-G8, G10		

3.5 Discussion

3.5.1 Comparison with other CMs identification methods

As is referred in the introduction, the most popular method for CMs identification is the largest angle gap (LAG) method which is widely used in SIMB based methods such as EEAC and SIME. This method can identify the CMs with the information of generator angles at a certain time soon after the clearance of disturbances. However, the time for information selection is not easy to decide. If the time is too early, the angles of generators are similar, as a result of which the CMs identification result is greatly influenced by the initial state. In this case, the CMs identification result will be inaccurate. On the other hand, if the time is too late, transient stability detection will be delayed. Literature [28] adopts the identification time as 100ms after the disturbance elimination, but the accuracy of CMs identification still can't be guaranteed. Moreover, the identification result of the conventional LAG method is fixed for each case and it fails to track the change of CMs during the dynamic process.

Inspired by the measurement-based coherency identification methods, the conventional LAG method can be modified to apply in real-time[5]. To eliminate the influence of the initial state, the same initialization proceeding as PTV methods is necessary. The clustering process is carried out at each moment with PMU information and CMs identification result is updated in real-time. This real-time LAG method has better performance than the conventional LAG method because it can identify the changes of CMs during the dynamic. For example, the change of CMs in case 2 and case 3 can also be identified by

the real-time LAG method. However, it leads to some new troubles. As it is shown in Figure 3-8, the application of the real-time LAG method in case 1 is not ideal. There is some confusion area for the modified LAG method where the CMs swing back and the angles of CMs are similar to that of NMs. The CMs identified by the real-time LAG method is not accurate at that time.

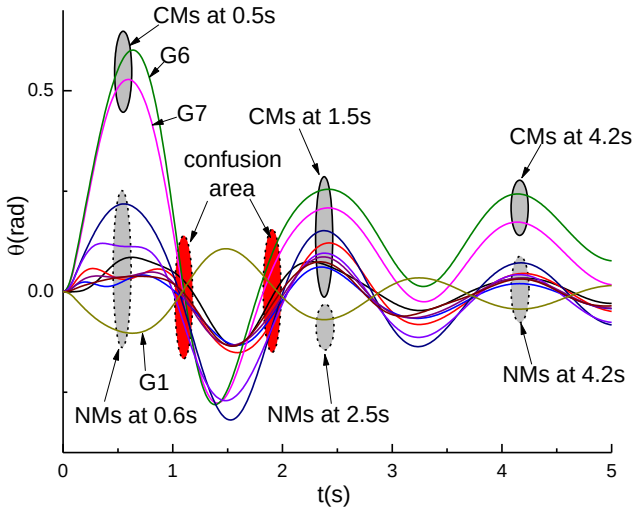

Figure 3-8 The real-time largest angle gap method for CMs identification

Table 3-4 Comparison of PTV method with other methods for CMs identification in Case 1

Time	t=0.6s	t=1.2s	t=2.5s	t=4.2s
Conventional LAG method	CMs:{G2-G9} NMs:{G1,G10}			
Real-time LAG method	CMs:{G6,G7} NMs:{G1-G5,G8-G10}	CMs:{ G4-G7 } NMs:{ G1-G3,G8-G10 }	CMs:{G2-G10} NMs:{G1}	CMs:{G6,G7} NMs:{G1-G5,G8-G10}
PTV method	CMs:{G2-G10} NMs:{G1}	CMs:{G2-G10} NMs:{G1}	CMs:{G2-G10} NMs:{G1}	CMs:{G2-G10} NMs:{G1}
Correct CMs and NMs	CMs: {G2-G10} NMs: {G1}			

The comparison of the conventional LAG method, real-time LAG method and proposed PTV method are presented in Table 3-4. The correct CMs of case 1 are always {G2-G10} from observation. However, the CMs identification result of the conventional LAG method is fixed as {G2-G9}, which is of course not correct. Although the real-time LAG method identifies the CMs correctly at 2.5s, it fails to identify the correct CMs at 0.6s and 4.2s. The identification results in the confusion area in Figure 3-8 are even worse when CMs swing back. On the contrary, the proposed PTV method correctly identifies the CMs at all these moments. The PTVs in Figure 3-2show obvious differences between CMs and NMs, especially

in the confusion area. Results in Table 3-4 indicate the feature matrix of PTVs are useful to distinguish the CMs and NMs.

3.5.2 The real-time identification for CMs

In general, the CMs are not identified in real-time in literature because the E-SMIB based methods are usually applied in offline transient stability analysis. Even in the online application, the CMs are identified once after disturbances clearance and the CMs identification result is fixed for each case. As a result, changes in CMs during the dynamic are ignored in these studies. With the development of WAMS in the power system, researchers try to extend the E-SMIB based methods to real-time transient stability detection and control. Motivated by this aim, the method of EEAC is developed to the DEEAC[71] and SIME method is developed to the predictive SIME method. Real-time prediction and parameters update is the key to obtain an accurate real-time E-SMIB. The method of CMs identification, as the first step of E-SMIB, also need to be improved to apply in the real-time scenario.

The real-time identification of CMs puts forwards a high request to the identification method with fast computation, less information requirement, and high accuracy. Proposed PTVs method succeeds in meeting these requirements:

a) The computation of PTVs and the K-means clustering are simple and fast. The average calculation time of tests cases of IEEE 39 bus 10 machine power system is **3ms** including the data processing and k-means clustering. The calculation is done with MATLAB R2013a on a computer with Intel i5 CPU. The results are believed to be further improved on a better computation platform.

b) For each moment, only two sample points of all generators are necessary to obtain all the PTVs. The necessary information includes the angle δ and angular speed $\Delta\omega$. These variables can be obtained directly or indirectly from PMUs. For example, the angles of generators δ are provided by PMUs. And the angular speed $\Delta\omega$ is computed by the output frequency f_i of generators from PMUs:

$$\Delta\omega_i = \frac{\omega_i - \omega_0}{\omega_0} = \frac{f_i - f_0}{f_0} \tag{3.6}$$

In (3.6), f_0 is the synchronization frequency of power system, i.e. 50Hz or 60Hz. And then δ and $\Delta\omega$ are further processed by (3.1) and (3.2) to obtain the angle θ and angular speed $\Delta\tilde{\omega}$ relative to the COI. The less requirement for information makes the method more reliable.

3.6 Summary

In this chapter, a PTV based real-time CMs identification scheme is proposed for TSA. This method is based on the PTVs, of which the feature matrix is used to describe the dynamic of generators. K-means

clustering method is used to separate the generators into two groups: CMs and NMs on the basis of the feature matrix. The PTVs are obtained with PMU information and the identification result is updated in real-time. The simulations in test system show that the proposed method is more accurate than conventional methods in general cases. Moreover, the PTV based method can track the time-evolution of CMs during the dynamic process. Combined with E-SIMB based method such as EEAC and SIME, this real-time CMs identification method will facilitate the study of real-time transient stability detection and control.

4 PTV Based Dynamic GCI Scheme for Controlled Islanding

Controlled islanding is regarded as the last control measure to protect the power system from severe blackouts. Three critical issues need to be addressed regarding the controlled islanding: when to initiate the islanding (the start-up criterion), where to separate the grid (the islanding strategy), and how to maintain the stability of islands after the separation (islands adjustment). To address the problem of "where", the constraint of generator coherency should be put in the first place.

The difficulty of the work of GCI for controlled islanding lies in three aspects. Firstly, it needs to track the variations of generator coherency accurately. Secondly, the GCI should be achieved rapidly at any moment that the controlled islanding starts. Thirdly, the coherency identification of non-generator buses, which is exactly the boundary of controlled islands, should be addressed.

To address these problems, a PTV based dynamic GCI scheme is proposed for controlled islanding in this chapter. The PTVs are firstly used to describe the dynamics of generators during the transient process. Then the hierarchical clustering algorithm is applied to determine the coherency of generators based on the feature matrix of PTVs. Next, inspired by PTVs on the Phase Plane for Generators (PPG), a novel concept of phase plane for buses (PPB) is proposed and used to determine coherency of non-generator buses. The PTV based GCI scheme for controlled islanding is given finally and verified in the IEEE 39-bus 10-machine power system.

4.1 Hierarchical clustering for GCI

To identify the dynamic coherency with the aid of PTVs, two problems need to be addressed, that is, how to compare the similarity of PTVs correctly and how to determine the number of coherent groups. Different from the problems of CMs identification in chapter 3, the GCI for controlled islanding has unlimited numbers of coherent groups. In this regard, the hierarchical clustering is applied in this chapter due to its high accuracy and no limits on cluster numbers. It consists of the following three steps:

Step 1: feature matrix formation. This step is to find the similarity or dissimilarity between every pair of generators at moment t. As discussed in chapter 2, the feature matrix is given in (2.6) and normalized in (2.7).

Step 2: hierarchical cluster tree formation. In this step, the Euclidean Distance is adopted to measure the distance between generator pair *i* and *j*, shown in (4.1).

$$dist(\vec{V}_{is}, \vec{V}_{js}) = \left\| \vec{V}_{is} - \vec{V}_{js} \right\|_2 \tag{4.1}$$

The cluster tree is formed step by step as follows.

(1) Each generator is an independent cluster.

(2) The nearest clusters with minimum distance are clustered into a new cluster. For example, if the distance between cluster *p* and *q* is minimum, then cluster *p* and *q* form a new cluster *r*.

(3) Thirdly, the distances from other clusters to the new cluster is re-calculated by the nearest neighbor:

$$dist(r,s) = \min(dist(x_{ri}, x_{sj})), i \in (1,...n_r),\ j \in (1,...n_s) \tag{4.2}$$

In (4.2), n_r is the number of generators in the new cluster *r* and x_{ri} is the *i*-th generator in cluster *r*. n_s is the number of generators in the other cluster *s* and x_{sj} is the *j*-th generator in cluster *s*.

(4) Return to (2) and form a new cluster with minimum distance until all generators belong to one cluster.

(5) Draw the dendrogram of the cluster tree.

Step 3: cluster number determination. This step is to determine the number of generator coherent groups based on the cluster tree. A threshold is set as 0.8 for cutting the cluster tree into groups. Coherent groups are formed when a node and all its sub-nodes have inconsistent values less than the threshold value.

4.2 PTV based generator coherency identification scheme

The overall procedure for dynamic coherency identification of generators consists of the following steps:

Step 1: Input the necessary information. Necessary information includes the angle and speed of each generator are input from PMUs at each moment.

Step 2: Form PTVs and compute feature matrix $\mathbf{A_s}$. The PTVs are formed with two moments of data ($t - \Delta t$ and t). The matrix is obtained by (2.6) and further normalized by(2.7).

Step 3: Identify coherent groups. The coherent groups are identified as section 4.2 by the hierarchical clustering method.

Step 4: Loop. Return to step 1 and begin new identification with data of the next moment.

It should be noted that the coherency identification only requires basic measurement information of generators, independent of system conditions and disturbances. It can self-adapted to different situations.

What's more, the time-rolling operation of proposed scheme ensures that the dynamic evolution of coherent groups can be tracked during the whole process.

4.3 Coherency identification of non-generator buses

To determine the controlled islands, the non-generator buses need to be assigned to corresponding coherent generators groups. A straight idea is to compute the electrical distances from non-generator buses to generator groups and assign them to the nearest generator groups. To compute the electrical distance, all the buses should be put in the same state space. The dynamics of generators are well expressed in the conventional phase plane; however, the non-generator buses cannot do like this. To this end, a special "phase plane" for all the buses is proposed where the x-axis is the voltage angle θ and the y-axis is the frequency *f*. These two state variables satisfy (4.3)[34].

$$f(t)=\frac{1}{2\pi f_0}\frac{\theta(t)-\theta(t-\Delta t)}{\Delta t} \tag{4.3}$$

where f_0 is the system nominal frequency and θ is the voltage phase angle of buses.

From (4.3), f is the derivative of θ on the phase plane for the buses (PPB), which is similar to the relation between $\Delta\omega$ and δ on the phase plane for generators (PPG). In other words, the proposed PPB can also describe the dynamic behaviors of the power system, the same as PPG. Moreover, all buses can be drawn on the PPB, which can be used to determine the association of non-generator buses and coherent generator groups. To simplify the computation, only the location information of buses on the PPB is used to determine the association of buses as follows.

step 1. Compute the centers of generator groups (COGGs). For example, the center phase point, $(\theta_{C,p}, f_{C,p})$, of coherent generator group *p* is computed by(4.4).

$$\theta_{C,p}=\frac{\sum_{i\in p}\theta_i}{N_p},\ f_{C,p}=\frac{\sum_{i\in p}f_i}{N_p} \tag{4.4}$$

where θ_i, f_i are the voltage angle and frequency of generator buses that belong to coherent group *p*, and N_p is the number of generator buses in this group. If there are *m* groups of coherent generators, we can obtain *m* COGGs in this step.

step 2. Standardize the state variables. To balance the weight of variables on PPB, we apply standardization to all non-generator buses and COGGs as (4.5) shows.

$$\theta^s=\frac{\theta}{\theta_{\max}},\ f^s=\frac{f}{f_{\max}} \tag{4.5}$$

where $\theta_{\max} = \max\{\theta_{C,1}, \theta_{C,2}, ..., \theta_{C,m}\}$, $f_{\max} = \max\{f_{C,1}, f_{C,2}, ..., f_{C,m}\}$ and m is the number of COGGs.

step 3. Compute the distance from non-generator buses to each COGG. In this paper, the Euclidean distance is used to compare the electrical distance. For the non-generator bus i, the distance to COGG p is obtained by (4.6).

$$d_{i,p} = \sqrt{\left(\theta_i^s - \theta_{C,p}^s\right)^2 + \left(f_i^s - f_{C,p}^s\right)^2} \tag{4.6}$$

It is noted that the distance from bus i to different COGGs should be computed, respectively. If there are m COGGs, the distances should be computed as $d_{i,1}, d_{i,2}, ..., d_{i,m}$.

step 4. Assign the non-generator buses to the nearest COGG. The non-generator bus i is assigned to the group q if it satisfies (4.7).

$$d_{i,q} = \min\{d_{i,1}, d_{i,2}, ..., d_{i,m}\} \tag{4.7}$$

step 5. Repeat steps 3 and 4 until all non-generator buses have already been assigned to corresponding coherent generator groups.

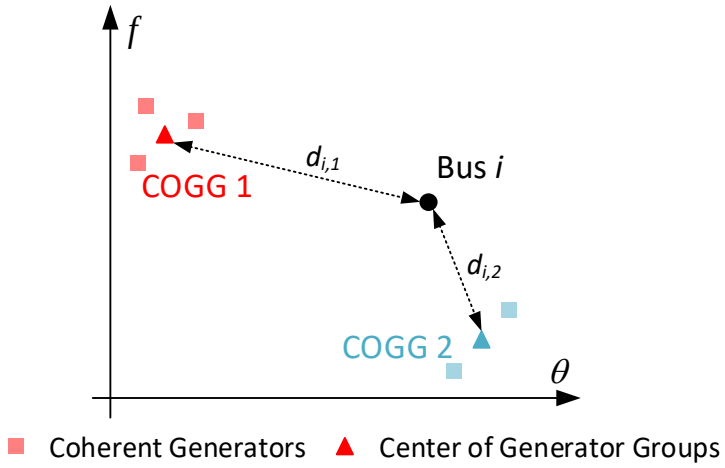

Figure 4-1 The association of non-generator bus i and coherent generator groups on the phase plane for the buses (PPB)

Figure 4-1 explains the association of non-generator buses and coherent generator groups. For the given case in the figure, two groups of coherent generators have been identified by the PTV method. Thus, two COGGs are firstly computed by (4.4). After the standardization by (4.5), the distances from non-generator bus i to two COGGs are computed by (4.6) as $d_{i,1}$ and $d_{i,2}$, respectively. The bus i is finally assigned to group 2 because $d_{i,2} < d_{i,1}$. The assignment of non-generator buses is highly efficient because it only takes little computation, which facilitates the fast determination of controlled islanding strategy. Meanwhile, the principle of "minimum electrical distance" ensures that each island composed of coherent

generators and associated non-generator buses is connected in topology, which is the guarantee of an effective controlled islanding strategy.

4.4 Flowchart of the PTV based GCI scheme for CI

The flowchart of the proposed dynamic GCI scheme for controlled islanding is given in Figure 4-2. There're 5 steps in this scheme.

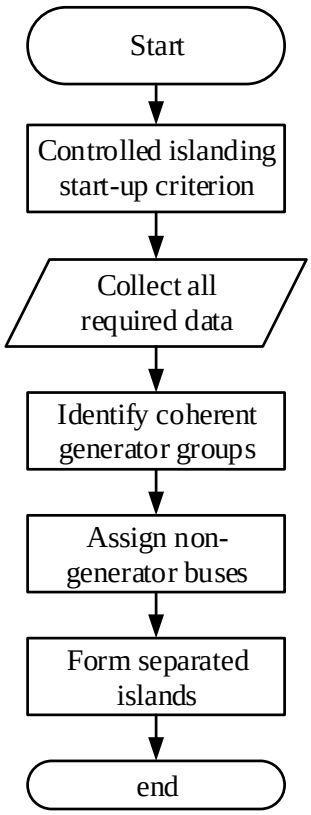

Figure 4-2 Flowchart of the proposed scheme

step 1. Initiate the scheme by the grid operator's instructions or the preset start-up criterion.

step 2. Collect the data including the state variables for all generators and all buses from PMUs. The required data include the power angle and rotor speed of all generators and the voltage angle and frequency of all buses. If the start-up time is t, the data of t and $t+\Delta t$ are required.

step 3. Identify the coherent generator groups with the PTV methods proposed in section 4.2.

step 4. Assign the non-generator buses to the coherent generator groups with the method proposed in section 4.3.

step 5. Intentionally disconnect certain transmission lines to form the separated islands based on the identified electrical areas.

4.5 Cases study

The IEEE 39-bus 10-machine power system is selected to verify the effectiveness of the proposed scheme. The required data includes the power angle and rotor speed of all generators, and the frequency and voltage angle of all buses. These transient responses of the power system are simulated on the PSASP-a platform for power system transient simulation and analysis. In the simulation, the two-axis generator model is adopted, and each generator is equipped with the automatic voltage regulators (AVRs) and Power System Stabilizers (PSSs). The simulated data input the proposed scheme as the real-time measurement data from the PMUs. The sample time interval, Δt, is 0.01s and the value of d_s to cut off the cluster tree is 1.

As it is pointed out in section 4.2, the proposed scheme aims to determine the controlled islanding strategy after the controlled islanding is initiated. The controlled islanding is initiated by the grid operator's instruction or preset start-up scheme. In this paper, an angle-threshold based start-up scheme is adopted as follows:

step:1 Collect required generators information from PMUs, including the power angle and speed deviation of all generators at time *t*;

step:2 Search for the maximum angle $\delta_{\max}(t)$ and the minimum angle $\delta_{\min}(t)$ at time *t*;

step:3 Compute the maximum angle difference $\Delta\delta_{\max}(t)$ at time *t* by $\Delta\delta_{\max}(t)=\delta_{\max}(t)-\delta_{\min}(t)$;

step:4 Compare $\Delta\delta_{\max}(t)$ with the preset angle threshold $\Delta\delta_{set}$. If $\Delta\delta_{\max}(t)>\Delta\delta_{set}$, controlled islanding strategy is then started. Otherwise, return to step 1 and continuously detect the out-of-step of the power system according to the measurement information of the next moment.

To fully examine the effectiveness of the proposed scheme, two different angle thresholds are used to launch the controlled islanding:

Start-up criterion 1: $\Delta\delta_{set}=\pi$.

Start-up criterion 2: $\Delta\delta_{set}=2\pi$.

Two cases are simulated for the verification. In each case, the proposed scheme will be tested twice because the scheme is initiated by two different criterions respectively.

4.5.1 Case 1

In case 1, a three-phase short-circuit ground fault occurs on line 27-28 at 0s and then the fault line is cleared at 0.2s. Generator angle curves of case 1 are given in Figure 4-3, which indicate G38 is out-of-step relative to other generators. The controlled islanding is initiated at t_{c1} (1.1s) by criterion 1 and at t_{c2} (1.4s) by criterion 2 respectively, which correspond to scenario 1 and 2.

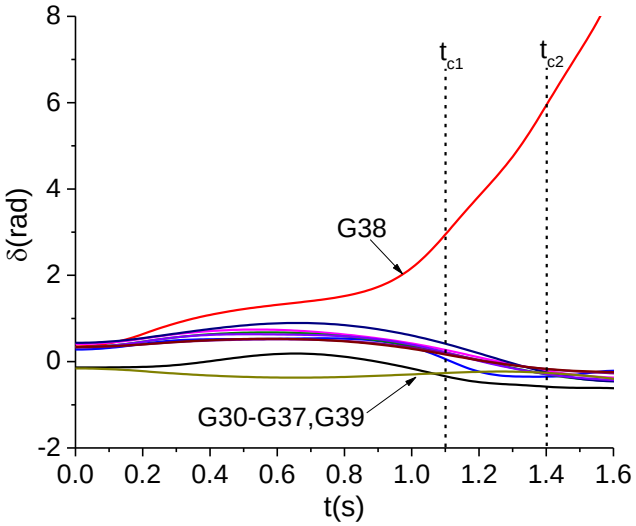

Figure 4-3 Angle Curves of All Generators in Case 1

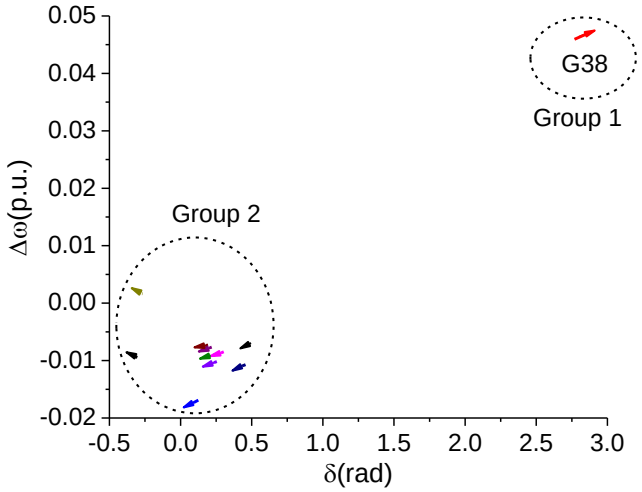

(a) Phase Plane for Generators (PPG) at 1.11s

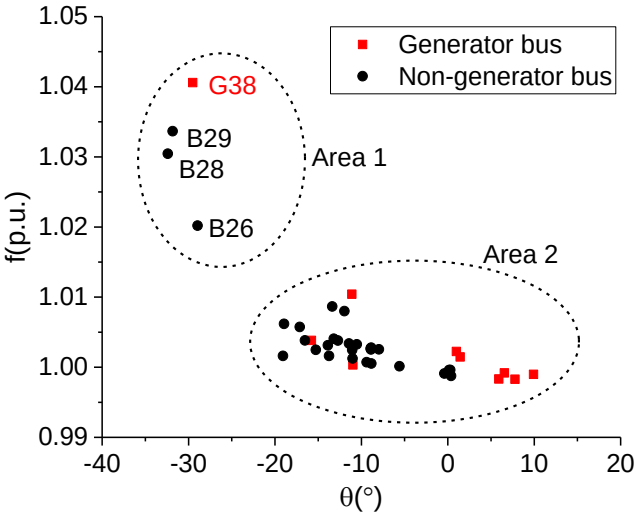

(b) Phase Plane for Buses (PPB) at 1.11s

Figure 4-4 PPG and PPB of Scenario 1 in case 1

In scenario 1, after the controlled islanding is initiated at 1.1s, the scheme immediately collects the data of generators and buses at time 1.1s and 1.11s. The power angle and speed deviation of generators are used to form the PTVs on the phase plane for generators (PPG). Then the PTV-based method is applied to identify the coherent generator groups. The feature matrix of scenario 1 is given in Table 4-1, on which generators are identified into two coherent groups: {G38} and {G30-G37, G39}. The coherent generator groups are shown vividly on the PPG in Figure 4-4(a). Afterward, the phase plane for buses (PPB) is built in Figure 4-4 (b) using the state variables of all buses at time 1.1s, and all non-generator buses are assigned to the coherent generator groups following the minimum distance principle. The identified coherent generators and areas of scenario 1 are given in Table 4-2. According to the results, the line 25-26 is disconnected intentionally to form the separated islands, as shown in Figure 4-6. Only requiring the data of two sampling moments after start-up, the proposed scheme correctly identifies the coherent generator groups and immediately determines the controlled islanding strategy after the start-up.

For scenario 2, Figure 4-5(a) gives the PTVs on the PPG and Table 4-2 gives the feature matrix, on which the coherent generators are identified based. Same coherent generator groups are obtained. Then the PPB is built in Figure 4-5(b) to assign the non-generator buses. The final coherent generators and areas of scenario 2 are the same as that of scenario 1. Despite started at different moments in two scenarios, the controlled islanding strategy is same in case 1.

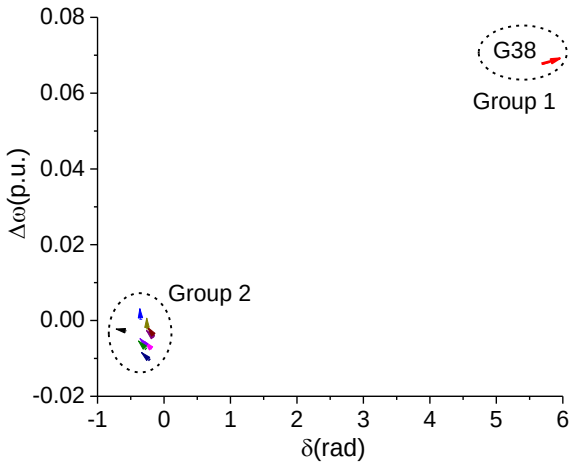

(a)Phase Plane for Generators (PPG) at 1.41s

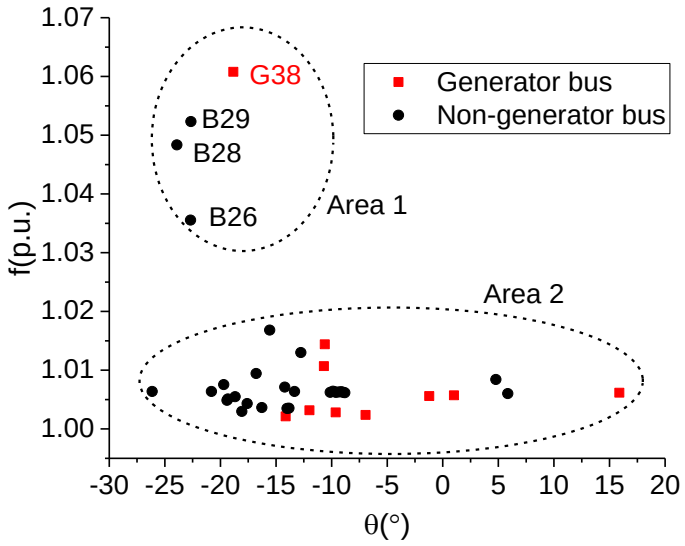

(b) Phase Plane for Buses (PPB) at 1.41s

Figure 4-5 PPG and PPB of Scenario 2 in Case 1

Table 4-1 Feature matrix A_s of Two Scenarios in Case 1

Gen. No.	Scenario 1			Scenario 2		
	δ_s	$\Delta\omega_s$	φ_s	δ_s	$\Delta\omega_s$	φ_s
G30	-0.6287	-0.71839	0.997249	-0.69291	-0.2498	0.998023
G31	0.351279	-5.70E-01	0.998446	-0.19353	-0.33822	0.992943
G32	0.400075	-0.60157	0.99765	-0.19738	-0.38508	0.994159
G33	0.460684	-0.8004	0.997245	-0.33258	-0.56191	0.99417
G34	0.854748	-0.84373	0.996915	-0.27795	-0.90054	0.995047
G35	0.444829	-0.70524	0.997247	-0.33686	-0.65121	0.995405
G36	0.562809	-0.66733	0.997089	-0.23784	-0.64502	0.995811
G37	0.181811	-1.33966	0.99578	-0.41996	0.0349	0.112423
G38	5.591963	3.627363	0.003429	7.001701	6.041884	0.001472
G39	-0.5231	1.26E-01	0.99	-0.3093	-0.19145	0.989821

Table 4-2 Coherent Generators and Areas of Two Scenarios in Case 1

Area	Coherent Generators	Associated Non-generator buses
1	38	26 28 29
2	30 31 32 33 34 35 36 37 39	1 2 3 4 5 6 7 8 9 10 11 12 13 14 15 16 17 18 19 20 21 22 23 24 25 27

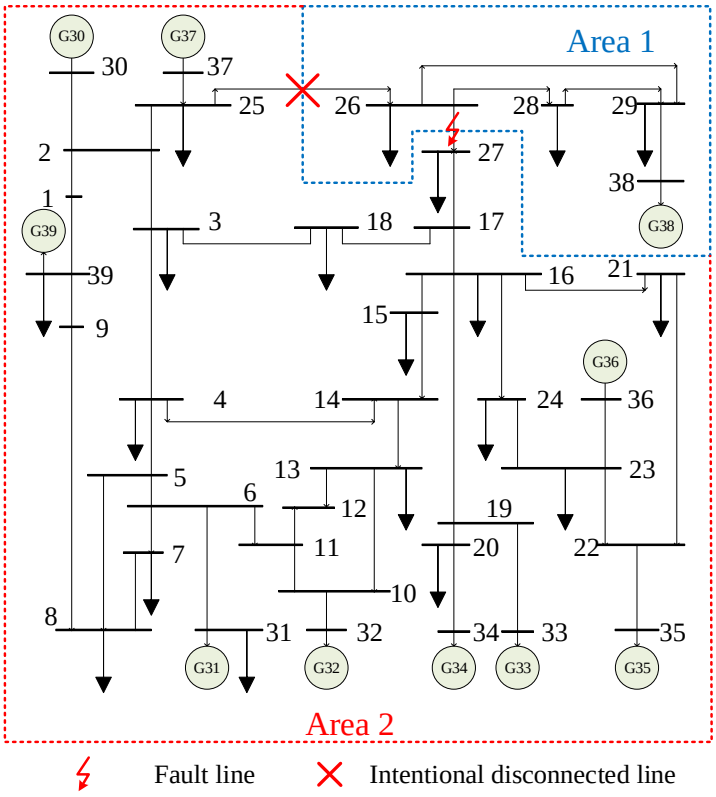

Figure 4-6 Areas Corresponding to Two Scenarios in Case 1

4.5.2 Case 2

In case 2, a three-phase short-circuit ground fault occurs on line 16-17 at 0s and then the fault line is cleared at 0.1s. Generator angle curves of case 2 are given in Figure 4-7, which indicate the oscillation mode of the system is changing with time. In the early stage, group {G31-G36} is out-of-step relative to the rest generators. However, as time goes on, {G31, G32} departs from the previous group and becomes a new group. The controlled islanding is initiated at t_{c1} (1.06s) by criterion 1 and at t_{c2} (1.37s) by criterion 2 respectively, which correspond to scenario 1 and 2.

In scenario 1, the generators are identified into two groups at 1.07s as {G31-G36} and {G30, G37-G39} based on the PTVs on the PPG in Figure 4-8(a). Then the non-generator buses are assigned to corresponding coherent generator groups by the phase points on the PPB in Figure 4-8 (b). The results of coherent generators and areas are given in Table 4-3. According to the results, line 3-4 and line 8-9 are disconnected intentionally to form separated islands, as shown in Figure 4-9.

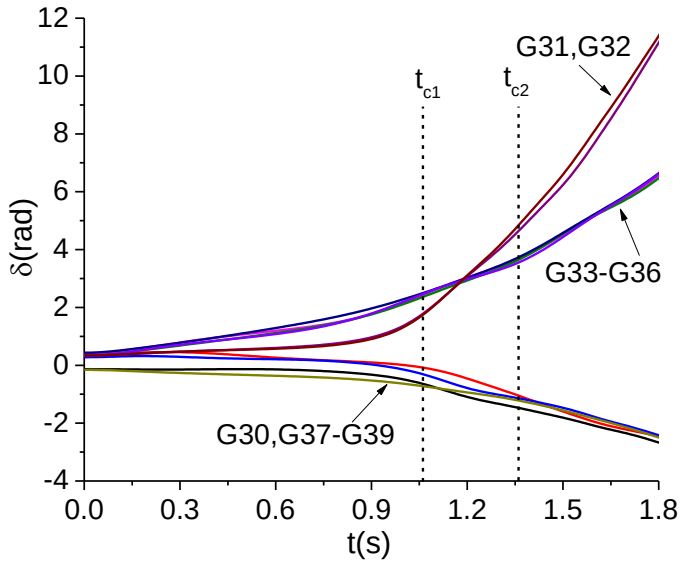

Figure 4-7 Angle Curves of All Generators in Case 2

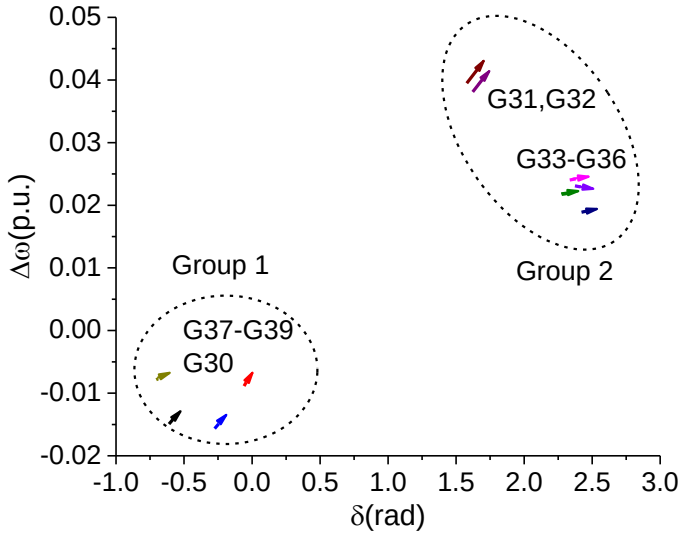

(a)Phase Plane for Generators (PPG) at 1.07s

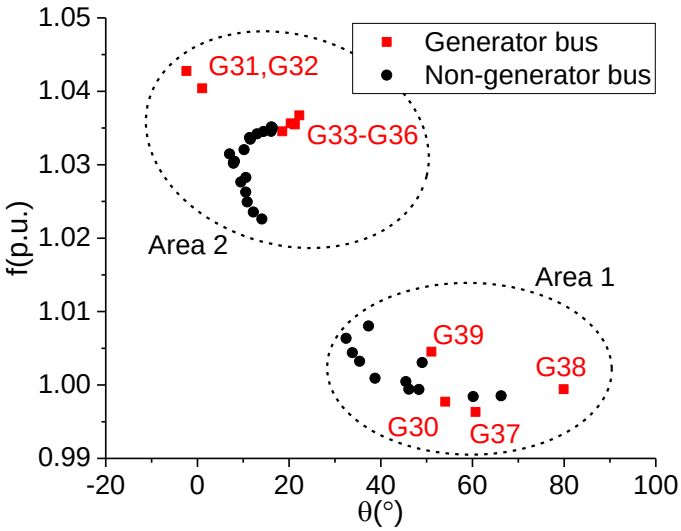

(b) Phase Plane for Buses (PPB) at 1.07s

Figure 4-8 PPG and PPB of Scenario 1 in case 2

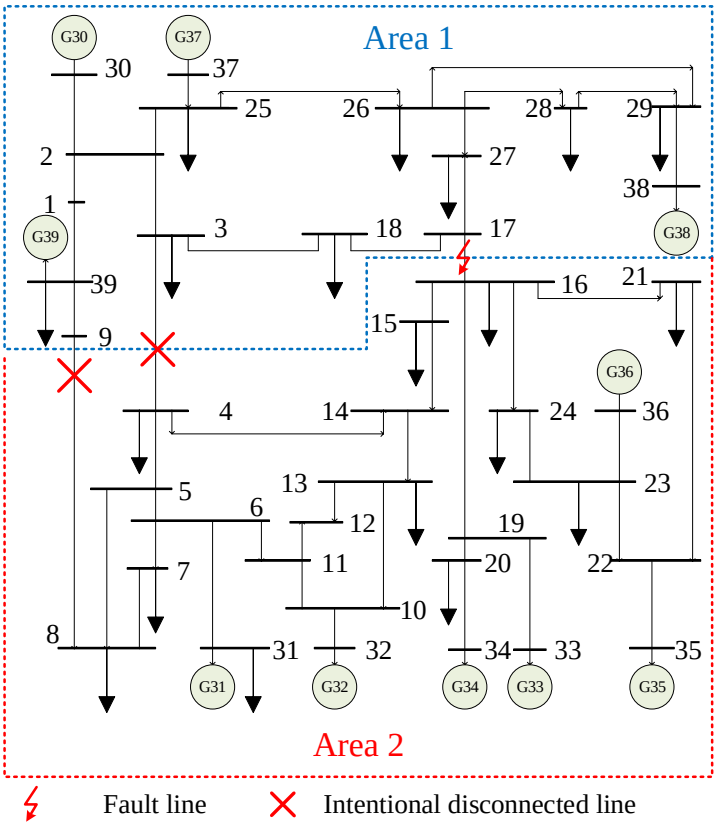

Figure 4-9 Areas Corresponding to Scenario 1 in Case 2

Table 4-3 Coherent Generators and Areas of Scenario 1 in Case 2

Areas	Coherent Generators	Associated Non-generator buses
1	30 37 38 39	1 2 3 9 17 18 25 26 27 28 29
2	31 32 33 34 35 36	4 5 6 7 8 10 11 12 13 14 15 16 19 20 21 22 23 24

In scenario 2, the controlled islanding strategy is, however, different. According to the PTVs on the PPG in Figure 4-10(a), the generators are identified into 3 groups: {G30, G37-G39}, {G31, G32} and {G33-G36}. Due to the changes in generator groups, the association of non-generator buses is also different from that in scenario 1. Based on the phase points of all buses on the PPB in Figure 4-10 (b), the power system is separated into three areas. The results of coherent generators and areas are given in Table 4-4. Line 3-4, line 8-9 and line 14-15 are disconnected to form the separated islands, as shown in Figure 4-11.

By the comparison of scenario 1 and 2 in case 2, it is demonstrated that the proposed scheme can correctly identify the dynamic coherency of generator groups. Due to the late start-up of controlled islanding in scenario 2, the oscillation is more severe than that in scenario 1, which leads to the change of coherent generators and areas. Based on the real-time measurement data, the proposed scheme tracks the

change of generator coherency and develops a controlled islanding strategy that is most suitable for the current situation.

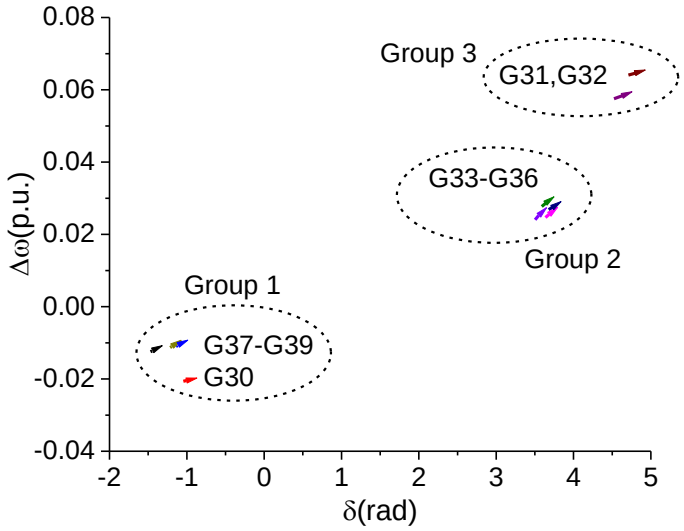

(a) Phase Plane for Generators (PPG) at 1.38s

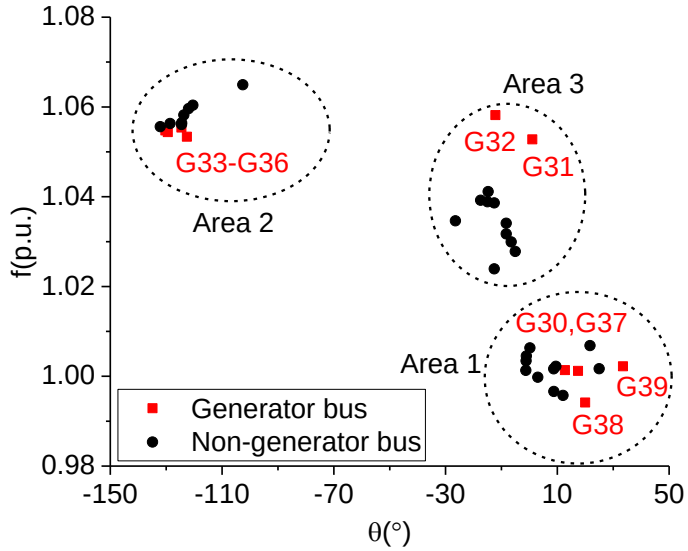

(b) Phase Plane for Buses (PPB) at 1.38s

Figure 4-10 PPG and PPB of Scenario 2 in case 2

Table 4-4 Coherent Generators and Areas of Scenario 2 in Case 2

Areas	Coherent Generators	Associated Non-generator buses
1	30 37 38 39	1 2 3 9 17 18 25 26 27 28 29
2	33 34 35 36	15 16 19 20 21 22 23 24
3	31 32	4 5 6 7 8 10 11 12 13 14

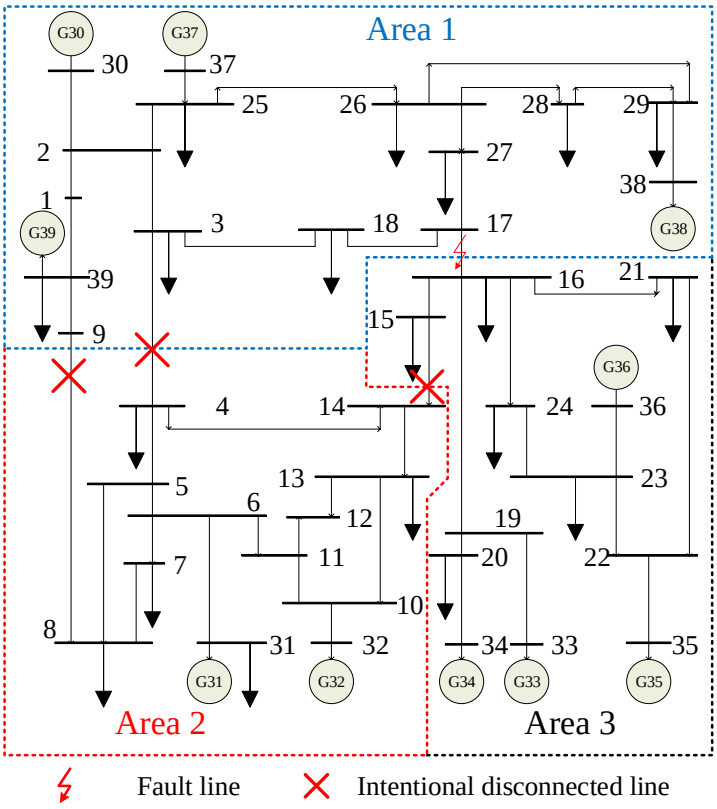

Figure 4-11 Areas Corresponding to Scenario 2 in Case 2

By the comparison of case 1 and 2, it is verified that the proposed scheme is adaptable to different disturbances and topology changes. Due to the difference in disturbances and the topology changes after the relay protection, the system shows different oscillation modes in these two cases. Independent on models and the information of fault and topology, the proposed scheme can develop different controlled islanding strategy for different cases.

4.6 Summary

In this chapter, a PTV based dynamic GCI scheme is proposed for controlled islanding. Firstly, the dynamics of generators are described by the PTVs on the PPG and the hierarchical clustering method is applied to determine the coherent groups. Then a PPB composed of bus voltage angle and frequency is built to assign the non-generator buses to the coherent groups. According to the identified coherent generators and areas, certain transmission lines are disconnected intentionally to form the separated islands. The case studies in the test system show that the proposed scheme can identify the dynamic generator coherency and make proper islanding strategy according to current system states.

5 Conclusions and Prospect

5.1 Conclusions

In this thesis, the PTV based dynamic GCI method and its application in power system transient stability assessment and control are studied. The main conclusions of the thesis are:

a) A profound analysis of the factors that influence GC is made based on the rotor motion equations of generators. The features of GC during the dynamic process are concluded as twofold: 1) the variation of GC to different operating conditions and disturbances, and 2) the time-evolution of GC. Based on the above analysis, a novel concept of PTV is proposed to address the problems of GCI. The advantages of the proposed PTVs are finally summarized into 5 aspects which includes adapting to different operating conditions and disturbances, providing abundant information for accurate and fast GCI, being able to tack the time-evolution of GC, flexible application and the efficient computation.

b) A PTV based real-time CMs identification scheme is proposed for TSA. In this scheme, PTVs are used to describe the dynamics of generators and K-means clustering algorithm is used to separate the generators into two groups: CMs and NMs. The PTVs are obtained based on PMU information and the results of CMs identification is updated in real-time. The simulations show that the proposed method is more accurate than conventional methods in general cases. Moreover, the PTV based method can track the time-evolution of CMs during the dynamic process.

c) A PTV based dynamic GCI scheme is proposed for controlled islanding. In this scheme, the dynamics of generators are described by the PTVs on the PPG and the hierarchical clustering method is applied to determine the coherent groups. A PPB composed of bus voltage angle and frequency is built to assign the non-generator buses to the coherent groups. According to the identified coherent generators and areas, certain transmission lines are disconnected intentionally to form the separated islands. The simulations show that the proposed scheme can identify the dynamic generator coherency and make proper islanding strategy according to current system states.

5.2 Prospect

This thesis only explores the works relative to generator coherency identification and doesn’t propose a comprehensive transient stability assessment scheme or controlled islanding scheme in chapters 4 and

5. Thus, future research prospects may include:

a) Real-time Transient Stability Assessment

The proposed PTV based CMs identification scheme has demonstrated its efficiency and accuracy in chapter 4, making it qualified to be used in the real-time TSA. Thus, research on the application of real-time TSA involved with PTVs worth further exploration.

b) Real-time Controlled Islanding Strategy

In chapter 4, the problem of "where" of controlled islanding seems to be addressed by the proposed scheme. However, this scheme requires the full-observability of the power system, which is difficult to implement in the present power system. Study on the application of the proposed method in scenarios that PMUs information is incomplete or with noises is required in the future.

Besides, how to maintain the stability of the islands after the separation is also a research focus. The proposed scheme ensures the coherency of generators on each island, which is the guarantee of angle stability. However, problems such as the frequency regulation caused by power imbalance remain unsolved.

References

[1] S. Yang, B. Zhang, M. Hojo, and F. Su, "An ME-SMIB Based Method for Online Transient Stability Assessment of a Multi-Area Interconnected Power System," *IEEE Access*, vol. 6, pp. 65874-65884, 2018.

[2] P. Kundur, J. Paserba, V. Ajjarapu, G. Andersson, A. Bose, C. Canizares, N. Hatziargyriou, D. Hill, A. Stankovic, and C. Taylor, "Definition and classification of power system stability," *IEEE transactions on Power Systems*, vol. 19, pp. 1387-1401, 2004.

[3] M. Ma, W. Jie, Z. Wang, and M. W. Khan, "Global Geometric Structure of the Transient Stability Regions of Power Systems," *IEEE Transactions on Power Systems*, p. 1-1, 2019-01-01 2019.

[4] A. M. Khalil and R. Iravani, "A Dynamic Coherency Identification Method Based on Frequency Deviation Signals," *IEEE Transactions on Power Systems*, vol. 31, pp. 1779-1787, 2016.

[5] F. Su, B. Zhang, S. Yang, and H. Wang, "Study on real-time clustering method for power system transient stability assessment," in *2016 IEEE Power and Energy Society General Meeting (PESGM)*, 2016, pp. 1-5.

[6] A. Raj, G. Gajjar and S. A. Soman, "Controlled islanding of transmission system using synchrophasor measurements," *IET Generation, Transmission & Distribution*, vol. 13, pp. 1942-1951, 2019-05-21 2019.

[7] O. Gomez and M. A. Rios, "Real time identification of coherent groups for controlled islanding based on graph theory," *IET Generation, Transmission & Distribution*, vol. 9, pp. 748-758, 2015.

[8] H. Verdejo, G. Montes, X. Olgui, and G. N, "Identification of coherent machines using modal analysis for the reduction of multimachine systems," *Latin America Transactions, IEEE (Revista IEEE America Latina)*, vol. 12, pp. 416-422, 2014-01-01 2014.

[9] C. Sturk, L. Vanfretti, Y. Chompoobutrgool, and H. Sandberg, "Coherency-Independent Structured Model Reduction of Power Systems," *IEEE Transactions on Power Systems*, vol. 29, pp. 2418-2426, 2014-01-01 2014.

[10] S. Wang, S. Lu, N. Zhou, G. Lin, M. Elizondo, and M. A. Pai, "Dynamic-Feature Extraction, Attribution, and Reconstruction (DEAR) Method for Power System Model Reduction," *IEEE Transactions on Power Systems*, vol. 29, pp. 2049-2059, 2014.

[11] W. Shaobu, L. Shuai, L. Guang, and Z. Ning, "Measurement-based coherency identification and aggregation for power systems," in *Power and Energy Society General Meeting, 2012 IEEE*, San Diego, CA, 2012, pp. 1-7.

[12] L. Mariotto, H. Pinheiro, G. Cardoso, A. P. Morais, and M. R. Muraro, "Power systems transient stability indices: an algorithm based on equivalent clusters of coherent generators," *IET Generation, Transmission & Distribution*, vol. 4, pp. 1223-1235, 2010-01-01 2010.

[13] S. R., E. M. and L. S., "A review of dynamic generator reduction methods for transient stability studies," in *2011 IEEE Power and Energy Society General Meeting*, 2011, pp. 1-8.

[14] Z. Lin, F. Wen, Y. Ding, Y. Xue, S. Liu, Y. Zhao, and S. Yi, "WAMS-based Coherency Detection for Situational Awareness in Power Systems with Renewables," *IEEE Transactions on Power Systems*, p. 1-1, 2018.

[15] Z. Lin, F. Wen, Y. Ding, and Y. Xue, "Wide-area coherency identification of generators in interconnected power systems with renewables," *IET Generation, Transmission & Distribution*, vol. 11, pp. 4444-4455, 2017-12-21 2017.

[16] A. Vahidnia, G. Ledwich, E. Palmer, and A. Ghosh, "Generator coherency and area detection in large power systems," *IET Generation, Transmission & Distribution*, vol. 6, pp. 874-883, 2012-01-01 2012.

[17] S. A. Siddiqui, K. Verma, K. R. Niazi, and M. Fozdar, "Real-Time Monitoring of Post-Fault Scenario for Determining Generator Coherency and Transient Stability Through ANN," *IEEE Transactions on Industry Applications*, vol. 54, pp. 685-692, 2018.

[18] C. Li, J. Xu and C. Zhao, "A coherency-based equivalence method for MMC inverters using virtual synchronous generator control," *IEEE Transactions on Power Delivery*, vol. 31, pp. 1369-1378, 2016.

[19] B. P. Padhy, S. C. Srivastava and N. K. Verma, "A coherency-based approach for signal selection for wide area stabilizing control in power systems," *IEEE Systems Journal*, vol. 7, pp. 807-816, 2013.

[20] M. R. Aghamohammadi and S. M. Tabandeh, "A new approach for online coherency identification in power systems based on correlation characteristics of generators rotor oscillations," *International Journal of Electrical Power & Energy Systems*, vol. 83, pp. 470-484, 2016.

[21] N. M. Manousakis, G. N. Korres and P. S. Georgilakis, "Taxonomy of PMU Placement Methodologies," *IEEE Transactions on Power Systems*, vol. 27, pp. 1070-1077, 2012.

[22] S. Yang, B. Zhang, M. Hojo, and K. Yamanaka, "An optimal scheme for PMU placement based on generators grouping," in *2016 IEEE PES Asia-Pacific Power and Energy Engineering Conference (APPEEC)*, 2016, pp. 2260-2264.

[23] M. H. Rezaeian Koochi, S. Esmaeili and G. Ledwich, "Locating minimum number of PMUs for pre- and post-disturbance monitoring of power systems," *IET Generation, Transmission & Distribution*, vol. 13, pp. 127-136, 2019-01-08 2019.

[24] W. Yu, Y. Xue, J. Luo, M. Ni, H. Tong, and T. Huang, "An UHV Grid Security and Stability Defense System: Considering the Risk of Power System Communication," *IEEE Transactions on Smart Grid*, vol. 7, pp. 491-500, 2016.

[25] Y. Xue, T. Van Custem and M. Ribbens-Pavella, "Extended equal area criterion justifications, generalizations, applications," *IEEE Transactions on Power Systems*, vol. 4, pp. 44-52, 1989-01-01 1989.

[26] T. Kyriakidis, G. Lanz, R. Cherkaoui, and M. Kayal, "A transient stability assessment method using post-fault trajectories," in *PowerTech (POWERTECH), 2013 IEEE Grenoble*, Grenoble, 2013, pp. 1-4.

[27] D. Ernst, D. Ruiz-Vega, M. Pavella, P. Hirsch, and D. Sobajic, "A Unified Approach to Transient Stability Contingency Filtering, Ranking, and Assessment," *IEEE Power Engineering Review*, vol. 21, pp. 71-72, 2001.

[28] M. Pavella, D. Ernst and D. Ruiz-Vega, *Transient stability of power systems: a unified approach to assessment and control*. Berlin, Germany: Springer Science & Business Media, 2012.

[29] S. Yang, B. Zhang, M. Hojo, and F. Su, "An ME-SMIB Based Method for Online Transient Stability Assessment of a Multi-Area Interconnected Power System," *IEEE Access*, vol. 6; 6, pp. 65874-65884, 2018-01-01.

[30] H. Xie, B. Zhang, G. Yu, Y. Li, P. Li, D. Zhou, and F. Yao, "Power System Transient Stability Detection Based on Characteristic Concave or Convex of Trajectory," in *Transmission and Distribution Conference and Exhibition: Asia and Pacific, 2005 IEEE/PES*, Dalian, 2005, pp. 1-6.

[31] H. Guo, H. Xie, B. Zhang, G. Yu, P. Li, Z. Bo, and A. Klimek, "Study on power system transient instability detection based on wide area measurement system," *EUROPEAN TRANSACTIONS ON ELECTRICAL POWER*, vol. 20, pp. 184-205, 2010.

[32] M. Dabbaghjamanesh, B. Wang, A. Kavousi-Fard, S. Mehraeen, N. D. Hatziargyriou, D. Trakas, and F. Ferdowsi, "A Novel Two-Stage Multi-Layer Constrained Spectral Clustering Strategy for Intentional Islanding of Power Grids," *IEEE Transactions on Power Delivery*, p. 1-1, 2019-01-01 2019.

[33] A. Esmaeilian and M. Kezunovic, "Prevention of Power Grid Blackouts Using Intentional Islanding Scheme," *IEEE Transactions on Industry Applications*, vol. 53, pp. 622-9, 2017.

[34] A. M. Khalil and R. Iravani, "A Dynamic Coherency Identification Method Based on Frequency Deviation Signals," *IEEE Transactions on Power Systems*, vol. 31, pp. 1779-1787, 2016.

[35] M. H. R. Koochi, S. Esmaeili and G. Ledwich, "Taxonomy of coherency detection and coherency-based methods for generators grouping and power system partitioning," *IET Generation, Transmission & Distribution*, vol. 13, pp. 2597-2610, 2019-01-01 2019.

[36] G. Xu and V. Vittal, "Slow coherency based cutset determination algorithm for large power systems," *IEEE Transactions on Power Systems*, vol. 25, pp. 877-884, 2010.

[37] A. M. Miah, "Study of a coherency-based simple dynamic equivalent for transient stability assessment," *IET Generation, Transmission & Distribution*, vol. 5, p. 405, 2011.

[38] X. Wang, V. Vittal and G. T. Heydt, "Tracing generator coherency indices using the continuation method: A novel approach," *IEEE Transactions on Power Systems*, vol. 20, pp. 1510-1518, 2005.

[39] M. A. M. Ariff and B. C. Pal, "Coherency Identification in Interconnected Power System—An Independent Component Analysis Approach," *IEEE Transactions on Power Systems*, vol. 28, pp. 1747-1755, 2013.

[40] R. Agrawal and D. Thukaram, "Support vector clustering-based direct coherency identification of generators in a multi-machine power system," *IET Generation, Transmission & Distribution*, vol. 7, pp. 1357-1366, 2013-01-01 2013.

[41] X. Qing, S. Wang, T. Jia, and Y. Niu, "Robust principal component analysis-based coherency identification of generators with missing PMU measurements," *IEEJ Transactions on Electrical and Electronic Engineering*, vol. 11, pp. 36-42, 2016.

[42] K. K. Anaparthi, B. Chaudhuri, N. F. Thornhill, and B. C. Pal, "Coherency Identification in Power Systems Through Principal Component Analysis," *IEEE Transactions on Power Systems*, vol. 20, pp. 1658-1660, 2005.

[43] F. Raak, Y. Susuki and T. Hikihara, "Data-Driven Partitioning of Power Networks Via Koopman Mode Analysis," *IEEE Transactions on Power Systems*, vol. 31, pp. 2799-2808, 2016.

[44] M. R. Arrieta Paternina, A. Zamora-Mendez, J. Ortiz-Bejar, J. H. Chow, and J. M. Ramirez, "Identification of coherent trajectories by modal characteristics and hierarchical agglomerative clustering," *Electric Power Systems*

Research, vol. 158, pp. 170-183, 2018.

[45] N. Senroy, "Generator coherency using the Hilbert – Huang transform," *IEEE Transactions on Power Systems*, vol. 23, pp. 1701-1708, 2008.

[46] Z. Lin, F. Wen, Y. Ding, and Y. Xue, "Data-Driven Coherency Identification for Generators Based on Spectral Clustering," *IEEE Transactions on Industrial Informatics*, vol. 14, pp. 1275-1285, 2018.

[47] R. Yadav, A. K. Pradhan and I. Kamwa, "A Spectrum Similarity Approach for Identifying Coherency Change Patterns in Power System due to Variability in Renewable Generation," *IEEE Transactions on Power Systems*, p. 1-1, 2019.

[48] F. Znidi, H. Davarikia, K. Iqbal, and M. Barati, "Multi-Layer Spectral Clustering Approach to Intentional Islanding In Bulk Power Systems," 2019.

[49] L. Ding, F. M. Gonzalez-Longatt, P. Wall, and V. Terzija, "Two-Step Spectral Clustering Controlled Islanding Algorithm," *IEEE Transactions on Power Systems*, vol. 28, pp. 75-84, 2013.

[50] S. Avdakovic, E. Becirovic, A. Nuhanovic, and M. Kusljugic, "Generator Coherency Using the Wavelet Phase Difference Approach," *IEEE Transactions on Power Systems*, vol. 29, pp. 271-278, 2014.

[51] S. Avdakovic, E. Becirovic, A. Nuhanovic, and M. Kusljugic, "Generator Coherency Using the Wavelet Phase Difference Approach," *IEEE Transactions on Power Systems*, vol. 29, pp. 271-278, 2014.

[52] S. Dasgupta, M. Paramasivam, U. Vaidya, and V. Ajjarapu, "PMU-Based Model-Free Approach for Real-Time Rotor Angle Monitoring," *IEEE Transactions on Power Systems*, vol. 30, pp. 2818-2819, 2015.

[53] T. Ishizaki, A. Chakrabortty and J. Imura, "Graph-Theoretic Analysis of Power Systems," *Proceedings of the IEEE*, vol. 106, pp. 931-952, 2018.

[54] W. Jin, D. Kundur and K. L. Butler-Purry, "A Novel Bio-Inspired Technique for Rapid Real-Time Generator Coherency Identification," *Smart Grid, IEEE Transactions on*, vol. 6, pp. 178-188, 2015-01-01 2015.

[55] T. Jiang, H. Jia, H. Yuan, N. Zhou, and F. Li, "Projection Pursuit: A General Methodology of Wide-Area Coherency Detection in Bulk Power Grid," *IEEE Transactions on Power Systems*, vol. 31, pp. 2776-2786, 2016.

[56] B. Zhang, "Strengthen the Protection Relay and Urgency Control Systems to Improve the Capability of Security in the Interconnected Power Network," Proceedings of CSEE, vol. 24, pp. 1-6, 2004.

[57] Y. Xue, "Space-time Cooperative Framework for Defending Blackouts Part I- From Isolated Defense Lines to Coordinated Defending," *Automation of Electric Power Systems*, pp. 8-16, 2006-01-10 2006.

[58] M. Yin, C. Y. Chung, K. P. Wong, Y. Xue, and Y. Zou, "An improved iterative method for assessment of multi-swing transient stability limit," *IEEE Transactions on Power Systems*, vol. 26, pp. 2023-2030, 2011.

[59] Y. Zhang, L. Wehenkel, P. Rousseaux, and M. Pavella, "SIME: A hybrid approach to fast transient stability assessment and contingency selection," *International Journal of Electrical Power & Energy Systems*, vol. 19, pp. 195-208, 1997.

[60] Y. Xue and M. Pavella, "Critical-cluster identification in transient stability studies," *IEE Proc. Gener. Transm. Distrib*, vol. 140, pp. 481-489, 1993.

[61] M. R. Salimian and M. R. Aghamohammadi, "Intelligent Out of Step Predictor for Inter Area Oscillations Using Speed-Acceleration Criterion as a Time Matching for Controlled Islanding," *IEEE Transactions on Smart Grid*, vol. 9, pp. 2488-2497, 2018.

[62] G. Isazadeh, A. Khodabakhshian and E. Gholipour, "New intelligent controlled islanding scheme in large interconnected power systems," *IET Generation, Transmission & Distribution*, vol. 9, pp. 2686-2696, 2015.

[63] Y. Cui, R. G. Kavasseri and S. M. Brahma, "Dynamic State Estimation Assisted Out-of-Step Detection for Generators Using Angular Difference," *IEEE Transactions on Power Delivery*, vol. 32, pp. 1441-1449, 2017.

[64] E. Farantatos, R. Huang, G. J. Cokkinides, and A. P. Meliopoulos, "A Predictive Generator Out-of-Step Protection and Transient Stability Monitoring Scheme Enabled by a Distributed Dynamic State Estimator," *IEEE Trans. Power Delivery*, vol. 31, pp. 1826-1835, 2016.

[65] B. Shrestha, R. Gokaraju and M. Sachdev, "Out-of-Step Protection Using State-Plane Trajectories Analysis," *IEEE Trans. Power Delivery*, vol. 28, pp. 1083-1093, 2013-01-01 2013.

[66] S. Paudyal, G. Ramakrishna and M. S. Sachdev, "Application of Equal Area Criterion Conditions in the Time Domain for Out-of-Step Protection," *IEEE TRANSACTIONS ON POWER DELIVERY*, vol. 25, pp. 600-609, 2010.

[67] Y. R. Rodrigues, M. Abdelaziz and L. Wang, "D-PMU Based Secondary Frequency Control for Islanded Microgrids," *IEEE Transactions on Smart Grid*, p. 1-1, 2019.

[68] Q. Wang, F. Li, Y. Tang, and Y. Xu, "Integrating Model-driven and Data-driven Methods for Power System Frequency Stability Assessment and Control," *IEEE Transactions on Power Systems*, p. 1-1, 2019.

[69] J. Tang, J. Liu, F. Ponci, and A. Monti, "Adaptive load shedding based on combined frequency and voltage stability assessment using synchrophasor measurements," *IEEE Transactions on Power Systems*, vol. 28, pp. 2035-2047, 2013.

[70] "IEEE 39-bus 10-machine power system model,". vol. 2019, 2019.

[71] Y. Xue, T. Huang, K. Li, D. Zhaoyang, Y. Dong, X. Feng, and H. Jie, "An efficient and robust case sorting algorithm for transient stability assessment," in *2015 IEEE Power & Energy Society General Meeting*, Denver, CO, USA, 2015, pp. 1-5.